國 立 交 通 大 學

電信工程學系碩士班

碩士論文

MIMO-OFDM 與 OFDM-CDMA 系統之頻率估計

Frequency Estimators for MIMO-OFDM and OFDM-CDMA Systems

研 究 生：江家賢　　Student: Jia-Shian Jiang

指導教授：蘇育德 博士　　Advisor: Dr. Yu Ted Su

公元 二００四 年 七 月

MIMO-OFDM 與 OFDM-CDMA 系統之頻率估計

Frequency Estimators

for MIMO-OFDM and OFDM-CDMA Systems

研 究 生：江家賢　　Student : Jia-Shian Jiang

指導教授：蘇育德 博士　　Advisor : Dr. Yu T. Su

國 立 交 通 大 學

電信工程學系碩士班

碩 士 論 文

A Thesis Submitted to
The Department of Communication Engineering
College of Electrical Engineering and Computer Science
National Chiao Tung University
In Partial Fulfillment of the Requirements
For the Degree of Master of Science
In
Communication Engineering
Hsinchu, 30056, Taiwan
June 2004

公元二００四年七月

MIMO-OFDM 與 OFDM-CDMA 系統之頻率估計

研究生：江家賢　　指導教授：蘇育德 博士

國立交通大學電信工程學系碩士班

中文摘要

正交分頻多工(Orthogonal Frequency Division Multiplexing, OFDM)技術近年來頗受到重視，其應用範圍也越來越廣。OFDM 通訊系統之設計必需要考慮到載波頻率偏移(CFO)補償這個重要的課題，因載波頻率偏移會破壞次載波的正交性且將大大的降低系統性能。在這篇論文裡，我們首先證明摩斯氏(Moose)和余氏(Yu)的最大可能頻率估計法可推廣到多輸出輸入正交分頻多工(MIMO-OFDM)系統的頻率估計，並有相當突出的性能表現。由於正交分頻多工分碼多重近接(OFDM-CDMA)很有可能成為下一代寬頻移動通訊的傳輸標準，而其頻率同步的問題尚少人探討，我們便接著研究這個頻率同步問題。我們考慮了非同步的上傳鏈路，其中每個用戶傳送的信號之時軸互不同步(timing asynchronous)，受到不同的通道衰褪並產生相異的頻率偏移。針對這樣的傳輸環境，頻率同步器的設計得要同時考慮多用戶干擾(multiple user interference, MUI)。我們先是應用多用戶偵測理論的最小輸出能量(minimum output energy, MOE)的法則，提出一種頻率估計法。這種方法需先計算相對每一個可能頻率偏移的最小輸出能量，接著再找出整個頻率不確定範圍內那一個頻率的 MOE 最大。因為這樣的搜尋複雜度高，於是我們進一步結合了陣列信號理論中尋向(directional finding)的概念，將原先的搜尋極大的最小輸出能量轉換成解多項式根的問題。我們提出的方法簡化了頻率同步演算法的複雜度且提高其性能表現。

Frequency Estimators for MIMO-OFDM and OFDM-CDMA systems

Student : Jia-Shian Jiang Advisor : Yu T. Su

The Department of Communication Engineering

National Chiao Tung University

Abstract

For orthogonal frequency division multiplexing (OFDM) based systems, a carrier frequency offset (CFO) existed between the transmitter and receiver will destroy the orthogonality of the subcarrier and degrades the performance. In this thesis, we extend both Moose's and Yu's maximum likelihood CFO estimation algorithm for multiple transmit and multiple receive MIMO-OFDM systems. OFDM Code-Divison Multiple-Access (OFDM-CDMA) have been one of the candidates for the next generation of mobile broadband communication. In an uplink, each user's transmitted signal suffers from asynchronous transmission and independent frequency selective channel and the different frequency offsets of each active user. We present a CFO estimation algorithm to be used in a asynchronous uplink and frequency selective channels for OFDM-CDMA systems. The algorithm estimates the CFO of the desired user and eliminates the multiuser interference (MUI). The CFO estimate is obtained by searching the value which maximizes the output energy of the minimum output energy (MOE) criterion. However, the CFO estimate requires an exhaustive search over the entire uncertainty range. We convert the min/max search into polynomial rooting problem.

誌 謝

本論文得以順利完成，首先要感謝我的指導教授蘇育德教授，在這兩年的研究生生活中，無論在電信領域的專業或生活上的待人處世，都使我有很大的收穫。也要感謝蒞臨的口試委員，他們提供的意見和補充資料使本文得以更加完整。另外，實驗室學長、同學及學弟妹的幫忙勉勵，讓我在學業及研究上獲益匪淺。

最後，要感謝的就是一直關心我鼓勵我的家人。

Contents

List of Figures

Chapter 1

Introduction

Orthogonal frequency division multiplexing (OFDM) is a popular modulation scheme for high-speed broadband wireless transmission [1], [2]. It popularity derives mainly from its capability to combat frequency selective fading as intersymbol interference (ISI) caused by multipath delay spread can be easily eliminated. By copying a properly selected portion (called a cyclic prefix) of an OFDM block and appending it to that block, each data-bearing subcarrier experiences only flat fading if the duration of the cyclic prefix is longer than the maximum channel delay spread and block length is smaller than the channel coherent time. Hence, complicated equalization can be replaced by an one-tap equalizer in frequency domain. OFDM has been adopted as the transmission scheme for industrial standards like the asymmetric digital subscriber line (ADSL), digital audio broadcasting (DAB), terrestrial digital video broadcasting (DVB-T), power-line transmission, and high-speed wireless broadband area networks (WLAN's). It is being considered, among others, for air interface standards in IEEE 802.15n personal area network and 4G mobile network. The former adopts the Multiple Input Multiple Output (MIMO) technique to enhance the capacity, where MIMO refers to systems that have multiple transmit antennas and multiple receive antennas. Depending on the MIMO channel condition, the capacity of MIMO system increases with the number of transmitter and receive antennas. Recent developments in MIMO techniques promise a great boost in performance for OFDM systems.

With all its merits, OFDM, however, is sensitive to the carrier frequency offset (CFO) caused by Doppler shifts or instabilities and mismatch between transmitter and receiver oscillators [3]. Depending on the application, the offset can be as large as many tens subcarrier spacing, and is usually divided into integer and fractional CFO parts. The presence of a fractional CFO causes reduction of amplitude of desired subcarrier and induces inter-carrier interference (ICI) because the desired subcarrier is no long sampled at the zero-crossings of its adjacent carriers' spectrum. If the fractional CFO part can be perfectly compensated, the residual integer CFO does not degrade the signal quality but still results in circular shifts of the desired output, causing decision errors.

There have been a multitude of proposals for CFO compensation. A maximum likelihood estimate was proposed by Moose [4], based on the observation of two consecutive and identical symbols. Its maximum frequency acquisition range is only $\pm 1/2$ subcarrier spacing because of mod 2π ambiguity. Two training symbols are also employed by Schmidl and Cox [5]. The first has two identical halves and serves to measure the frequency offset with an ambiguity equal to the subcarrier spacing. The second contains a pseudonoise sequence and its used to resolve the ambiguity i.e. estimate integer CFO. Morelli *et al,* [6] suugested an estimate based on the observation of two consecutive symbols. This method overcomes the the ambiguity due to phase uncertainty but requires heavier computational load.

Combining the advantages of OFDM and MIMO techniques, a variety of MIMO-OFDM architectures techniques have been proposed. Much less literature on the corresponding time and frequency synchronization and channel estimation issues can be found though [7], [8], [9]. The purpose of the first part of this thesis (Chapter 2) is find a more efficient solution for MIMO-OFDM frequency synchronization. We find it both feasible and convenient to extend two of the OFDM CFO ML estimation approaches to the MIMO scenario.

Multi-Carrier Code-Division Multiple-Access (MC-CDMA), as many authors had

shown [10], [11], [12], is an attractive multiple access technique for future mobile broadband communication, for it combines the advantages of OFDM and CDMA. Tureli *et al.* [13] proposed a low complexity blind CFO estimator for synchronous systems, exploiting the virtual subcarriers, regarded as redundancy, for estimate the CFO. Using orthogonal spreading codes and assuming uncorrelated channel responses, one can has an orthogonal effective channel spreading signatures. Multipath fading and time-asynchronous reception, however, destroy the orthogonality among different subcarriers and users's spreading codes. Takyu, Ohtsuki and Nakagawa [14] found that the MMSE-MUD (minimum mean squared error based multi-user detection) scheme can compensate most of the frequency offset effect if it is small. Seo and Kim (SK) [15] presented a blind CFO estimator for use in an asynchronous system in AWGN channels. Their estimate was obtained by searching for the value that maximizes the corresponding minimum output energy (MOE). In the second part of this thesis, we extend the SK approach, taking both multipath fading and time-asynchronous effects into account, and propose an efficient frequency synchronizer.

The rest of the thesis is organized as follows. In Chapter 2, we extend Moose's ML CFO estimation algorithm for use in a multiple-antenna environments, assuming two identical pilot symbols are available. We then extend the Yu's ML CFO estimation algorithm [16] that uses multiple repetitive pilot symbols. Chapter 3 presents our study on CFO estimation for asynchronous OFDM-CDMA systems in frequency selective fading based on the MOE criterion. We also investigate the feasibility of joint CFO and channel estimation and suggest some iterative approaches. Finally, in Chapter 4, we summary the major results of our effort and suggest some topics for future investigation.

Chapter 2

Carrier Frequency Offset Estimation for MIMO-OFDM Systems

2.1 Introduction

Fig. 2.1 plots a block diagram of a OFDM modulator where S/P and DAC are used to denote serial-to-parallel converter and digital-to-analog converter, respectively. The information symbols are used to modulate subcarriers via an N-point inverse discrete Fourier transform (IDFT). The output of the IDFT (IFFT) block is converted to a serial complex block and a cyclic prefix (CP) is added to each block. The total duration of an OFDM symbol (frame) is equal to the length of the CP plus that of the IDFT symbol block. The CP is a copy of the tail part of the time-domain OFDM block and is attached to the front of the block. As long as the duration of the CP is longer than the channel impulse response, intersymbol inference (ISI) can be eliminated by the receiver through frequency domain excision.

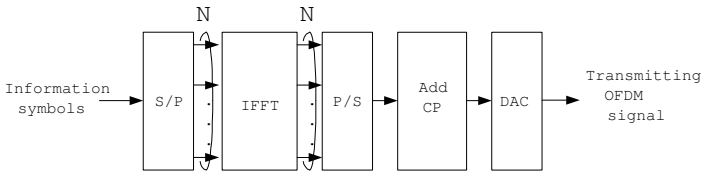

Figure 2.1: Block diagram of an OFDM modulator.

An OFDM demodulator is shown in Fig. 2.2. Based on the timing (frame) recovery

subsystem output, the baseband receiver removes the CP part, takes discrete Fourier transform (DFT) on the remaining part and then compensates for the CFO and channel effect using information given by the frequency synchronization and channel estimation units before making decision on symbols modulated on each subcarrier, if no soft-decision channel decoding is needed. Parallel-to-serial conversion can be performed either before or after making symbol decision (detection).

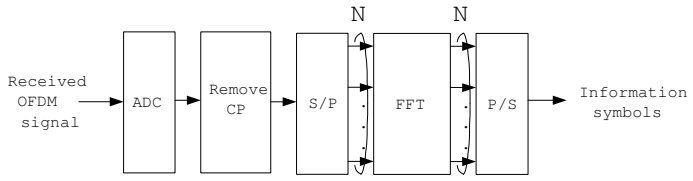

Figure 2.2: A typical OFDM demodulator.

Fig. 2.3 depicts a MIMO-OFDM system with M_T transmit antennas and M_R receive antennas. System design consideration prefer the choice of subcarrier spacing is such that each subcarrier suffers only slow flat fading. The resulting MIMO-OFDM channel can thus be characterized by a family of matrices whose members specify the space transmission characteristic, i.e., the (i, j) entry of a member matrix represents the channel response between the ith receive antenna and the jth transmit antenna associated with a subcarrier. One can also use a tensor to describe the space-frequency channel responses.

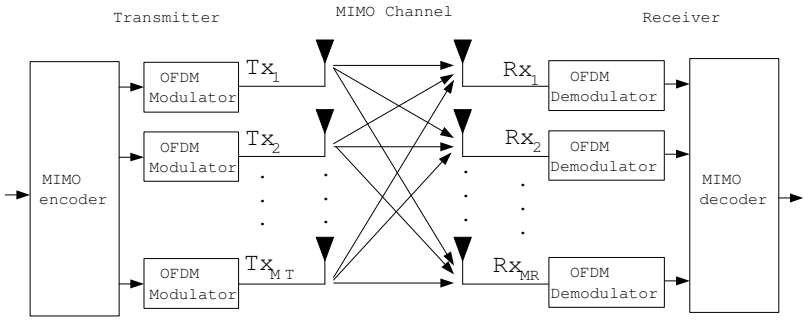

Figure 2.3: Block diagram of a typical MIMO-OFDM system.

The carrier frequency offset (CFO) is caused by (i) the time-varying nature of the transmission medium, (ii) the instabilities and mismatch between the transmitter and receiver oscillators and (iii) the relative movement between the transmitter and receiver. For all practical purpose, different transmit/receive RF branches of a MIMO system must be frequency-coherent, i.e., the transmitted carrier frequency and receiver frequency down-converters are each derived from a common frequency synthesizer, resulting in the model shown in Fig. 2.4.

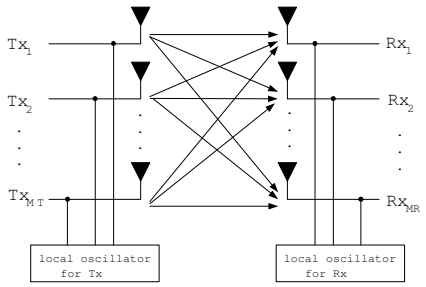

Figure 2.4: Frequency synthesizer model of a MIMO-CDMA system.

The cyclic prefix (CP) consists of N_g samples, which is supposed to be greater than or equal to the maximum relative delay that includes users' timing ambiguities and the maximum multipath delay; see Fig. 2.5. When this assumption is valid, the received time-domain sequence, after removing the CP part, is the circular convolution of the transmitted sequence with the channel impulse response plus white Gaussian noise.

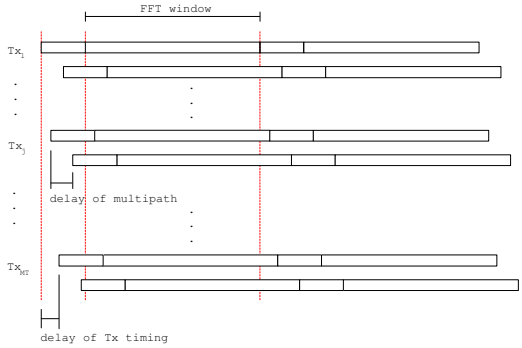

Figure 2.5: Timing assumption of the MIMO-OFDM receiver under consideration.

2.2 System Model

Consider a frequency selective fading channel associated with a MIMO system of M_T transmit and M_R receive antennas. The equivalent time-domain baseband signal at the output of the ith receive antenna, $y_i[n]$, is given by

$$y_i[n] = \sum_{j=1}^{M_T} r_{i,j}[n] + w_i[n];\ n = 1, 2, ..., N;\ i = 1, 2, ..., M_R \tag{2.1}$$

where $\{w_i[n]\}$ is a complex additive white Gaussian noise (AWGN) sequence and

$$r_{i,j}[n] = \frac{1}{N} \sum_{k \in D_j} \sqrt{\frac{E_s}{M_T}} S_j[k] H_{i,j}[k] e^{j2\pi n(k+\epsilon)/N} \tag{2.2}$$

is the part of the OFDM signal received by the ith receive antenna contributed by the jth transmit antenna. Moreover,

- $S_j[k]$ represents the symbol carried by the kth subcarrier at the jth transmit antenna.
- $H_{i,j}[k]$ is the channel transfer function between the ith receive antenna and the jth transmit antenna at the kth subcarrier.
- ϵ denotes the relative carrier frequency offset of the channel (the ratio of the actual frequency to the intercarrier spacing).
- D_j is the set of modulated subcarrier for the jth transmit antenna.
- E_s is the average energy allocated to the kth subcarrier evenly divided across the transmit antennas.
- $\{h_{i,j}[n]\}$ and $H_{i,j}[k] = \sum_{n=0}^{L-1} h_{i,j}[n] e^{-\frac{j2\pi kn}{N}}$ are the channel impulse and frequency response between the ith receive antenna and the jth transmit antenna at the kth subcarrier.
- L is the maximum channel memory of all $M_T M_R$ SISO component channels.

Fig. 2.6 plots the transmission channel model for the ith receive antenna with respect to the M_T transmit antennas. Rewriting (2.1) in matrix form

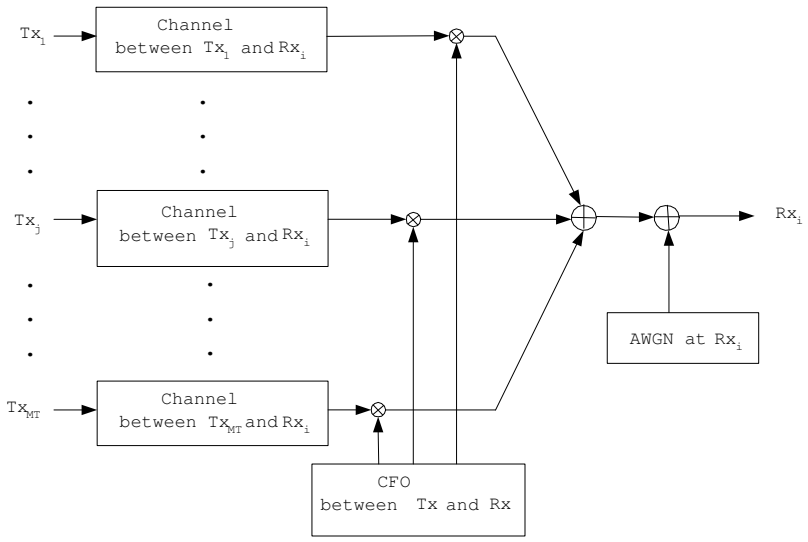

Figure 2.6: Channel model for the ith receive antenna.

$$\begin{pmatrix} y_1[n] \\ y_2[n] \\ \vdots \\ y_{M_R}[n] \end{pmatrix} = \frac{1}{N} \sum_{k \in D_j} \sqrt{\frac{E_s}{M_T}} \begin{pmatrix} H_{1,1}[k] & H_{1,2}[k] & \cdots & H_{1,M_T}[k] \\ H_{2,1}[k] & H_{2,2}[k] & \cdots & H_{2,M_T}[k] \\ \vdots & \vdots & \ddots & \vdots \\ H_{M_R,1}[k] & H_{M_R,2}[k] & \cdots & H_{M_R,M_T}[k] \end{pmatrix} \begin{pmatrix} S_1[k] \\ S_2[k] \\ \vdots \\ S_{M_T}[k] \end{pmatrix} e^{j2\pi n(k+\epsilon)/N} + \begin{pmatrix} w_1[n] \\ w_2[n] \\ \vdots \\ w_{M_R}[n] \end{pmatrix} \tag{2.3}$$

and using the substitutions,

$$\begin{aligned} \mathbf{y}[n] &= (y_1[n]\ y_2[n]\ \cdots\ y_{M_R}[n])^T \\ \mathbf{S}[k] &= (S_1[k]\ S_2[k]\ \cdots\ S_{M_T}[k])^T \\ \mathbf{H}[k] &= [H_{i,j}[k]] \\ \mathbf{w}[n] &= (w_1[n]\ w_2[n]\ \cdots\ w_{M_R}[n])^T \end{aligned}$$

we obtain

$$\mathbf{y}[n] = \frac{1}{N} \sum_{k \in D_j} \sqrt{\frac{E_s}{M_T}} \mathbf{H}[k]\mathbf{S}[k] e^{j2\pi n(k+\epsilon)/N} + \mathbf{w}[n] \tag{2.4}$$

Taking N-point DFT on both sides of the above equation leads to

$$\mathbf{Y}[k] = \sqrt{\frac{E_s}{M_T}} \sum_{m \in D_j} \mathbf{H}[m]\mathbf{S}[m] \left(\frac{1}{N} \sum_{n=0}^{N-1} e^{j2\pi(m+\epsilon)n/N} e^{-j2\pi kn/N} \right) + \mathbf{W}[k] \tag{2.5}$$

where $\mathbf{Y}[k] = (Y_1[k]\ Y_2[k]\ \cdots\ Y_{M_R}[k])^T$, $\mathbf{W}[k] = (W_1[k]\ W_2[k]\ \cdots\ W_{M_T}[k])^T$ and

$$\begin{aligned} Y_i[k] &= \sum_{n=0}^{N-1} y_i[n] e^{-\frac{j2\pi kn}{N}} \\ W_i[k] &= \sum_{n=0}^{N-1} w_i[n] e^{-\frac{j2\pi kn}{N}} \end{aligned}$$

Let ϵ_f and ϵ_i be respectively the fractional and integer parts of the CFO so that $\epsilon = \epsilon_f + \epsilon_i$ and define

$$\begin{aligned} \mathbf{Y}[k] &= \sqrt{\frac{E_s}{M_T}} \sum_{m \in D_j} \mathbf{H}[m]\mathbf{S}[m] \left(\frac{1}{N} \sum_{n=0}^{N-1} e^{j2\pi(m+\epsilon_f+\epsilon_i)n/N} e^{-j2\pi kn/N} \right) + \mathbf{W}[k] \\ &= \sqrt{\frac{E_s}{M_T}} \mathbf{H}[k-\epsilon_i]\mathbf{S}[k-\epsilon_i] \left(\frac{1}{N} \sum_{n=0}^{N-1} e^{j2\pi\epsilon_f n/N} \right) \\ &\quad + \sqrt{\frac{E_s}{M_T}} \sum_{\substack{m \in D_j \\ m \neq k-\epsilon_i}} \mathbf{H}[m]\mathbf{S}[m] \left(\frac{1}{N} \sum_{n=0}^{N-1} e^{j2\pi(m+\epsilon_i-k)n/N} e^{j2\pi\epsilon_f n/N} \right) + \mathbf{W}[k] \\ &= \sqrt{\frac{E_s}{M_T}} \underbrace{\mathbf{H}[k-\epsilon_i]\mathbf{S}[k-\epsilon_i]}_{circular\ shift} \underbrace{\left(\frac{1}{N} \frac{sin(\pi\epsilon_f)}{sin(\pi\epsilon_f/N)} e^{j\pi\epsilon_f(N-1)/N} \right)}_{reduction\ of\ the\ desired\ subcarrier's\ amplitude} \\ &\quad \underbrace{+ \sqrt{\frac{E_s}{M_T}} \sum_{\substack{m \in D_j \\ m \neq k-\epsilon_i}} \mathbf{H}[m]\mathbf{S}[m] \left(\frac{1}{N} \frac{sin(\pi(\epsilon_f+\epsilon_i))}{sin(\pi(m-k+\epsilon_f+\epsilon_i)/N)} e^{j\pi(\epsilon_f+\epsilon_i)(N-1)/N} e^{-j\pi(m-k)/N} \right)}_{ICI} \\ &\quad + \mathbf{W}[k]. \end{aligned} \tag{2.6}$$

It is clear that the presence of a fractional CFO causes reduction of the desired subcarrier's amplitude and induces inter-carrier interference (ICI). If the fractional CFO part can be perfectly compensated for, the integer CFO, if exists, will result in a circular shift of the desired output, causing decision errors.

2.3 Maximum Likelihood Estimate of CFO

2.3.1 Generalized Moose Estimate

Let $\mathcal{D}$ be the set of modulated subcarrier (indexes) that bear a pseudonoise (PN) sequence on the even frequencies and zeros on the odd frequencies. The resulting time-domain training sequence has two identical halves

$$\mathbf{r}[n] = \frac{1}{N}\sum_{k\in\mathcal{D}_e}\sqrt{\frac{E_s}{M_T}}\mathbf{H}[k]\mathbf{S}[k]e^{j2\pi n(k+\epsilon)/N};\ n=1,2,...,N/2 \tag{2.7}$$

$$\begin{aligned}\mathbf{r}[n+N/2] &= \frac{1}{N}\sum_{k\in\mathcal{D}_e}\sqrt{\frac{E_s}{M_T}}\mathbf{H}[k]\mathbf{S}[k]e^{j2\pi(n+\frac{N}{2})(k+\epsilon)/N}\\ &= \frac{1}{N}\sum_{k\in\mathcal{D}_e}\sqrt{\frac{E_s}{M_T}}\mathbf{H}[k]\mathbf{S}[k]e^{j2\pi n(k+\epsilon)/N}e^{j2\pi\frac{N}{2}(k+\epsilon)/N}\\ &= \mathbf{r}[n]e^{j2\pi\epsilon/2},\quad n=1,2,...,N/2\end{aligned} \tag{2.8}$$

where $\mathbf{r}[n] = (r_1[n]\ r_2[n]\ \cdots\ r_{M_R}[n])^T$ and $\mathcal{D}_e$ is the subset of even numbers in $\mathcal{D}$. Taking into account the AWGN term, we obtain

$$\mathbf{y}[n] = \mathbf{r}[n] + \mathbf{w}[n] \tag{2.9}$$

$$\mathbf{y}[n+N/2] = \mathbf{r}[n]e^{j2\pi\epsilon/2} + \mathbf{w}[n+N/2] \tag{2.10}$$

where $\mathbf{w}[n] = (w_1[n]\ w_2[n]\ \cdots\ w_{M_R}[n])^T$. As illustrated in Fig. 2.7, we define

$$\overline{\mathbf{y}}_1[i] = (y_i[1]\ y_i[2]\ \cdots\ y_i[N/2])$$

$$\overline{\mathbf{r}}_1[i] = (r_i[1]\ r_i[2]\ \cdots\ r_i[N/2])$$

$$\overline{\mathbf{w}}_1[i] = (w_i[1]\ w_i[2]\ \cdots\ w_i[N/2])$$

and

$$\overline{\mathbf{y}}_2[i] = (y_i[N/2+1]\ y_i[N/2+2]\ \cdots\ y_i[N])$$

$$\overline{\mathbf{r}}_2[i] = (r_i[N/2+1]\ r_i[N/2+2]\ \cdots\ r_i[N])$$

$$\overline{\mathbf{w}}_2[i] = (w_i[N/2+1]\ w_i[N/2+2]\ \cdots\ w_i[N])$$

where the subscript indicates either the first or the second half of a time-domain OFDM frame and the indexes within the bracket denotes from which receive antenna the time domain sample is derived.

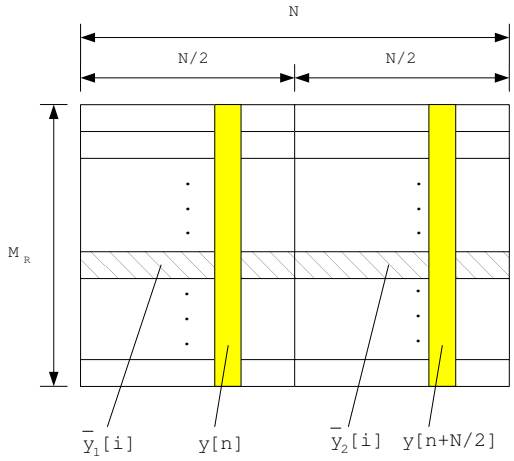

Figure 2.7: Definitions of various vector notations.

(2.9) and (2.10) then have the simplified expressions

$$\overline{\mathbf{y}}_1[i] = \overline{\mathbf{r}}_1[i] + \overline{\mathbf{w}}_1[i] \tag{2.11}$$

$$\overline{\mathbf{y}}_2[i] = \overline{\mathbf{r}}_1[i]e^{j2\pi\epsilon/2} + \overline{\mathbf{w}}_2[i] \tag{2.12}$$

The ML estimate of the parameter ϵ, given the received vector $(\overline{\mathbf{y}}_1[i], \overline{\mathbf{y}}_2[i])$, is obtained by maximizing the likelihood function

$$f(\overline{\mathbf{y}}_1[i], \overline{\mathbf{y}}_2[i]|\epsilon) = f(\overline{\mathbf{y}}_2[i]|\overline{\mathbf{y}}_1[i], \epsilon) f(\overline{\mathbf{y}}_1[i]|\epsilon) \tag{2.13}$$

where we have denoted various conditional probability density functions by similar functional expressions, $f(\cdot|\cdot)$. As ϵ gives no explicit information about $\overline{\mathbf{y}}_1[i]$, i.e. $f(\overline{\mathbf{y}}_1[i]|\epsilon) = f(\overline{\mathbf{y}}_1[i])$, the ML estimate of ϵ is given by

$$\widehat{\epsilon} = \arg\max_{\epsilon}[f(\overline{\mathbf{y}}_2[i]|\overline{\mathbf{y}}_1[i], \epsilon) f(\overline{\mathbf{y}}_1[i]|\epsilon)] = \arg \max_{\epsilon}[f(\overline{\mathbf{y}}_2[i]|\overline{\mathbf{y}}_1[i], \epsilon)] \tag{2.14}$$

Since

$$\overline{\mathbf{y}}_2[i] = (\overline{\mathbf{y}}_1[i] - \overline{\mathbf{w}}_1[i])e^{j2\pi\epsilon/2} + \overline{\mathbf{w}}_2[i] = \overline{\mathbf{y}}_1[i]e^{j2\pi\epsilon/2} + (\overline{\mathbf{w}}_1[i] - \overline{\mathbf{w}}_2[i]e^{j2\pi\epsilon/2}) \tag{2.15}$$

and $\overline{\mathbf{w}}_1[i]$, $\overline{\mathbf{w}}_2[i]$ are temporally white Gaussian with zero mean and variance $\sigma_w^2\mathbf{I}$, where $\mathbf{I}$ is the identity matrix, the multivariate Gaussian vector $\overline{\mathbf{y}}_2[i]$ have mean $\overline{\mathbf{y}}_1[i]e^{j2\pi\epsilon/2}$ and covariance matrix

$$E[(\overline{\mathbf{w}}_2[i]-\overline{\mathbf{w}}_1[i]e^{j2\pi\epsilon/2})(\overline{\mathbf{w}}_2[i]-\overline{\mathbf{w}}_1[i]e^{j2\pi\epsilon/2})^H] \;=\; 2\sigma_w^2\mathbf{I} \tag{2.16}$$

Then

$$\Lambda(\epsilon) = f(\overline{\mathbf{y}}_1[1]\ \cdots\overline{\mathbf{y}}_1[M_R],\ \overline{\mathbf{y}}_2[1]\ \cdots\overline{\mathbf{y}}_2[M_R]|\overline{\mathbf{y}}_1[1]\ \cdots\overline{\mathbf{y}}_1[M_R],\epsilon) \tag{2.17}$$

$$\begin{aligned}
&\propto \exp\left\{-\frac{1}{2\sigma_w^2}\sum_{i=1}^{M_R}\left(\overline{\mathbf{y}}_2[i]-\overline{\mathbf{y}}_1[i]e^{j2\pi\epsilon/2}\right)\left(\overline{\mathbf{y}}_2[i]-\overline{\mathbf{y}}_1[i]e^{j2\pi\epsilon/2}\right)^H\right\}\\
&\propto \exp\left\{\frac{1}{2\sigma_w^2}\sum_{i=1}^{M_R}2\Re\{\overline{\mathbf{y}}_2[i]\overline{\mathbf{y}}_1^H[i]e^{-j2\pi\epsilon/2}\}\right\}\\
&= \exp\left\{\frac{1}{\sigma_w^2}\Re\left\{\left(\sum_{i=1}^{M_R}\sum_{n=1}^{N/2}y_i^*[n]y_i[n+N/2]\right)e^{-j2\pi\epsilon/2}\right\}\right\}
\end{aligned} \tag{2.18}$$

The ML estimate of ϵ is given by

$$\begin{aligned}
\widehat{\epsilon} &= \arg\max_{\epsilon}\Lambda(\epsilon)\\
&= \frac{1}{\pi}\mathrm{Arg}\left(\sum_{i=1}^{M_R}\sum_{n=1}^{N/2}y_i^*[n]y_i[n+N/2]\right)
\end{aligned} \tag{2.19}$$

where $\mathrm{Arg}(x)$ is the principal argument of the complex number x. In summary, the generalized Moose estimate for two identical halves pilot symbols of length N_W and N_D-spaced, as shown in Fig. 2.8, is given by

$$\widehat{\epsilon} \;=\; \frac{N}{2\pi N_D}\mathrm{Arg}\left(\sum_{i=1}^{M_R}\sum_{n=1}^{N_W}y_i^*[n]y_i[n+N_D]\right) \tag{2.20}$$

The range of this estimator is $\pm\frac{N}{2N_D}$ subcarrier spacings.

2.3.2 Extended Yu Estimate

Consider a MIMO-OFDM system that uses multiple identical pilot symbols. After discarding the first received symbol, the remaining K pilot symbols at the ith receive

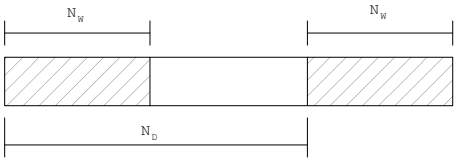

Figure 2.8: The N_D-spaced estimator.

antenna, $y_i(k,m)$, can be represented as

$$y_i(k,m) = x_i(k,m) + w_i(k,m) \tag{2.21}$$

for $k = 1, \cdots, K$ and $m = 1, \cdots, M$ where $x_i(k,m)$ is the mth sample of the kth (time-domain) symbol of the channel output at the ith receive antenna. $\{w_i(k,m)\}$ are uncorrelated circularly symmetric Gaussian random variables at the ith receive antenna (rv's) with zero mean and variance $\sigma_w^2 = E\{|w_i(k,m)|^2\}$. Note that

$$x_i(k,m) = x_i(1,m)e^{j2\pi(k-1)M\epsilon/N} \tag{2.22}$$

where ϵ is the relative frequency offset of the channel (i.e., the true frequency offset divided by the intercarrier spacing). Let

$$Y_i(m) = [y_i(1,m) \ \cdots \ y_i(K,m)]^T \tag{2.23}$$

$$A(\epsilon) = \left[1 \ e^{j2\pi\epsilon M/N} \ \cdots \ e^{j2\pi\epsilon(K-1)M/N}\right]^T \tag{2.24}$$

$$W_i(m) = [w_i(1,m) \ \cdots \ w_i(K,m)]^T \tag{2.25}$$

where $(\cdot)^T$ denote the matrix transpose. $Y_i(m)$, $A(\epsilon)$ and $W_i(m)$ are vectors of dimension $K \times 1$. Then, as shown in Fig. 2.9, we have

$$Y_i(m) = A(\epsilon)x_i(1,m) + W_i(m), \quad m = 1, \cdots, M \tag{2.26}$$

The received samples can thus be expressed compactly as

$$\mathbf{Y}_i = A(\epsilon)X_i + \mathbf{W}_i, \tag{2.27}$$

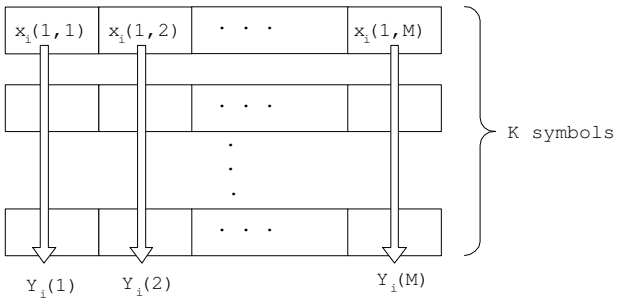

Figure 2.9: Symbol arrangement and definitions of the extended Yu's ML estimate at the ith receive antenna.

where $\mathbf{Y}_i = [Y_i(1) \ \cdots \ Y_i(M)]$ is an $K \times M$ matrix, $X_i = [x_i(1,1) \ \cdots \ x_i(1,M)]$ is an $1 \times M$ vector and $\mathbf{W}_i = [W_i(1) \ \cdots \ W_i(M)]$ is an $K \times M$ matrix. Since the noise is temporally white Gaussian, $Y_i(m)$ is a multivariate Gaussian distributed random vector with covariance matrix $\sigma_w^2 I$. The joint ML estimates of A and X_i, treating X_i as a deterministic unknown vector, are obtained by maximizing the following joint likelihood function :

$$f(\mathbf{Y}_1 \ \cdots \ \mathbf{Y}_{M_R} | A, X_1 \ \cdots \ X_{M_R}) = \prod_{i=1}^{M_R} \prod_{m=1}^{M} f(Y_i(m)|A, x_i(1,m))$$
$$\propto e^{-1/\sigma_w^2 \sum_{i=1}^{M_R} \sum_{m=1}^{M} ||Y_i(m) - Ax_i(1,m)||^2}$$

The corresponding log-likelihood function, after dropping constant and unrelated terms, is given by

$$\Lambda(A, x_i(1,m)) = \sum_{i=1}^{M_R} \sum_{m=1}^{M} ||Y_i(m) - Ax_i(1,m)||^2 \tag{2.28}$$

For a given A, setting $\nabla_{x_i(1,m)} ||Y_i(m) - Ax_i(1,m)||^2 = 0$, we obtain the conditional ML estimate, $\hat{x}_i(1,m) = x_{LS_i}(1,m) = A^+ Y_i(m)$, where $A^+ = A^H/K$ and H denotes the Hermitian operation. By substituting the least-square solution, $x_{LS_i}(1,m)$, we obtain

$$\begin{aligned}
\Lambda(A) &= \sum_{i=1}^{M_R} \sum_{m=1}^{M} ||Y_i(m) - AA^+ Y_i(m)||^2 = \sum_{i=1}^{M_R} \sum_{m=1}^{M} ||P_A^\perp Y_i(m)||^2 \\
&= \sum_{i=1}^{M_R} \sum_{m=1}^{M} Y_i^H(m) P_A^\perp Y_i(m) = tr\left(P_A^\perp \sum_{i=1}^{M_R} \sum_{m=1}^{M} Y_i(m) Y_i^H(m) \right) \\
&= M_R M tr(P_A^\perp \hat{R}_{YY})
\end{aligned} \tag{2.29}$$

where $tr(\cdot)$ denotes the trace of a matrix, $\hat{R}_{YY} \stackrel{def}{=} \frac{1}{M_R M}\sum_{i=1}^{M_R}\sum_{m=1}^{M} Y_i(m)Y_i^H(m)$, and $P_A^{\perp} \stackrel{def}{=} I - AA^{+}$. The desired CFO estimate is then given by

$$\hat{\epsilon} = \arg\{\min_{\epsilon}\ tr(P_A^{\perp}\hat{R}_{YY})\} = \arg\{\max_{\epsilon}\ tr(P_A\hat{R}_{YY})\} = \arg\{\max_{\epsilon}\ A^H\hat{R}_{YY}A\} \quad (2.30)$$

Invoking an approach similar to that used by the MUSIC algorithm, we set $z = e^{j2\pi\epsilon M/N}$ and define the parametric vector

$$A(z) = \left[1\ z\ z^2\ \cdots\ z^{K-1}\right]^T, \quad (2.31)$$

so that the log-likelihood $\Lambda = A^H\hat{R}_{YY}A$ can be expressed as a polynomial of order $2K-1$,

$$\Lambda(z) = A(z)^H\hat{R}_{YY}A(z) = \sum_{n=-(K-1)}^{K-1} s(n)z^n, \quad (2.32)$$

where $s(n) = \sum_{i,j}\hat{R}_{YY}(i,j)$, for $n = j-i$, and $n = -K+1, \cdots, K-1$. As the log-likelihood is a real smooth function of ϵ, taking derivative of $\Lambda(e^{j2\pi\epsilon M/N})$ with respect to ϵ and setting $\partial\Lambda(e^{j2\pi\epsilon M/N})/\partial\epsilon \stackrel{def}{=} \dot{\Lambda}(\epsilon) = 0$, we obtain

$$F(z) - F^*(z) = 0, \quad (2.33)$$

where $F(z) = \sum_{n=1}^{K-1} ns(n)z^n$ is a polynomial of order $K-1$. If $\{z_i\}$ are the nonzero complex roots of $\dot{\Lambda}(z)$ then the desired estimate is given by

$$\hat{\epsilon} = \frac{N}{j2\pi M}\ln\hat{z}, \quad (2.34)$$

where

$$\hat{z} = arg\{\max_{z_i}\Lambda(z)\}. \quad (2.35)$$

We summarize the above ML estimation procedure as following.

1. Collect K received symbols from all receive antennas and construct the sample correlation matrix $\hat{R}_{YY}$, $\hat{R}_{YY} = \frac{1}{M_R M}\sum_{i=1}^{M_R}\sum_{m=1}^{M} Y_i(m)Y_i^H(m)$.

2. Calculate the coefficients of $F(z)$ based on $\hat{R}_{YY}$ where $F(z) = \sum_{n=1}^{K-1} ns(n)z^n$, $s(n) = \sum_{i,j} \hat{R}_{YY}(i,j)$, for $n = j - i$.

3. Find the nonzero unit-magnitude roots of $F(z) - F^*(z) = 0$.

4. Obtain the CFO estimate from $\hat{\epsilon} = \frac{N}{j2\pi M} \ln \hat{z}$ and $\hat{z} = arg\{\max \Lambda(z)\}$ where $\Lambda(z) = A(z)^H \hat{R}_{YY} A(z)$, $A(z) = \left[1 \; z \; z^2 \; \cdots \; z^{K-1}\right]^T$, $z = e^{j2\pi\epsilon M/N}$.

The range of our estimator is $\pm\frac{N}{2M}$ subcarrier spacings.

2.4 Simulation Results and Discussion

The computer simulation results reported in this section are obtained by using a pilot format the same as the IEEE 802.11a standard with a sample interval of 50 ns. The frequency-selective fading channel has sixteen paths with independent complex Gaussian distributed amplitudes and a exponentially decaying power delay profile with rms delay spreads of 50 ns. The tap coefficients are normalized such that the sum of the average power per channel is unity. The DFT size is $N = 64$. The signal-to-noise ratio (SNR), defined as the ratio of the received signal power (from all M_T transmitters) to the noise power at the ith receive antenna, is assumed to be the same for each receive antenna. For Moose estimate, the training part consists of two identical halves with length $N_W = 32$. The range of CFO estimator is ± 1 subcarrier spacings. Fig. 2.10 shows the performance of generalized Moose CFO estimate for different number of transmit and receive antennas. Obviously, the MSE performance improves as the number of receive antennas, M_R, increases. Fig. 2.11 presents the performance of extended Yu estimate for different number of transmit and receive antennas. The training symbol has two identical halves with $K = 2$ and $M = 32$. The range of CFO estimator is ± 1 subcarrier spacings. For training symbol with two identical repetition, the performance of extended Yu estimate is the same as the performance of generalized Moose's CFO estimate. Fig. 2.12 plots the performance of generalized Moose's CFO estimate with

two identical halves with length $N_W = 32$ for different number of transmit and receive antennas. Similarly, the performance of CFO estimates is an increasing function of the number of the receive antennas. We divide roughly into four groups. The first group is $M_R = 1, M_T = 1, 2, 4, 8$, the second is $M_R = 2, M_T = 1, 2, 4, 8$ and so on. For first group, the performance of CFO estimate with $M_R = 1, M_T = 8$ is better than with $M_R = 1, M_T = 1$ duo to transmit diversity. The last group with $M_R = 8$ is more close together than the first group with $M_R = 1$ duo to receive diversity. The performance of CFO estimate for the second group, $M_R = 2$, is roughly 3dB better than for the first group, $M_R = 1$, duo to two receive antennas received double energy than single receive antenna. Fig. 2.13 shows the performance of extended Yu estimate and generalized Moose estimate. The training symbols have 4 repetitions with $K = 4$ and $M = 16$. The training symbols for generalized Moose estimate are length $N_W = 32$ i.e. take first two training symbols as one training symbol and take last two training symbols as one training symbol. The range of generalized Moose's CFO estimator is ± 1 subcarrier spacings. The range of extended Yu estimator is ± 2 subcarrier spacings. For 4 repetitions, the performance of extended Yu estimate is better than generalized Moose estimate because extend Yu estimate use all information of training symbols.

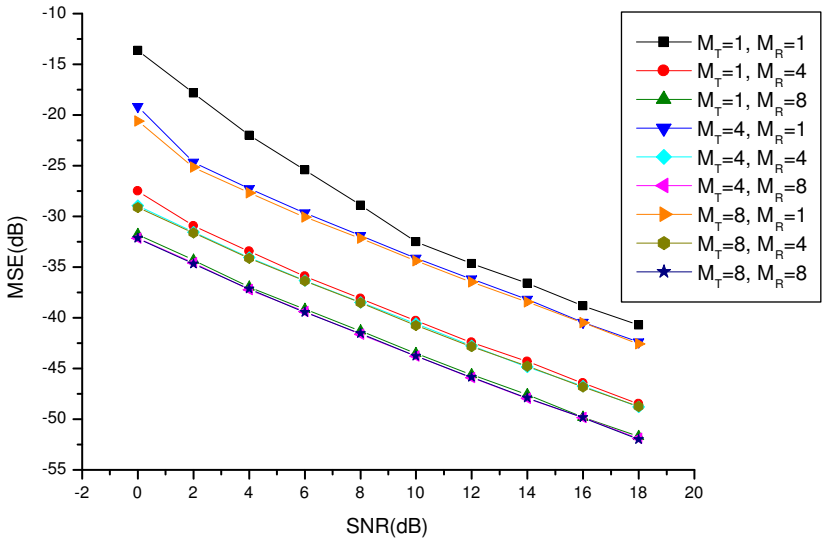

Figure 2.10: MSE performance of generalized moose estimate for two repetitions, true CFO=0.7 subcarrier spacings.

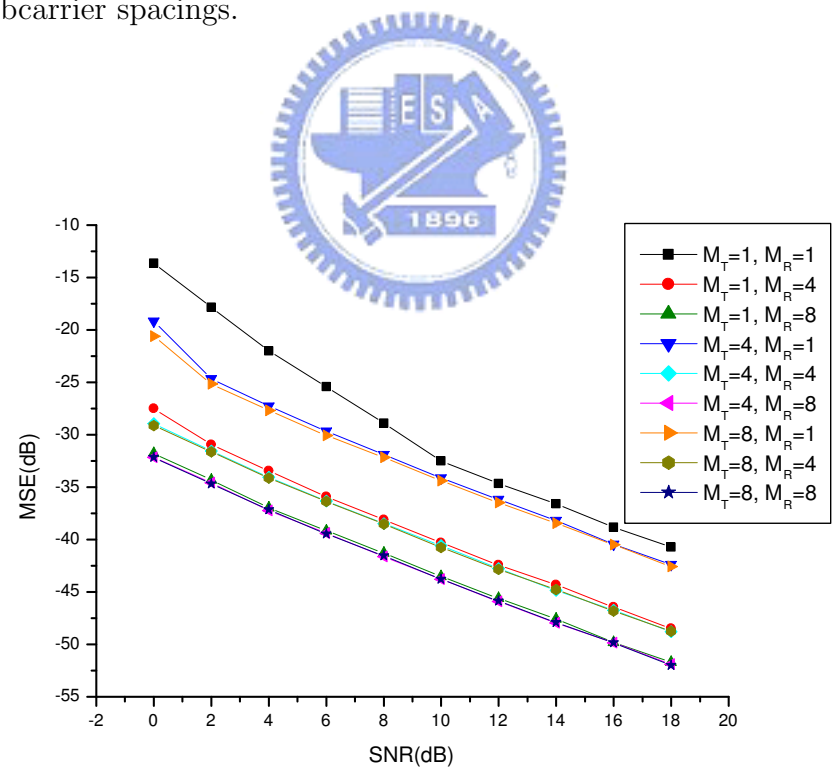

Figure 2.11: MSE performance of extended Yu estimate for two repetitions, true CFO=0.7 subcarrier spacings.

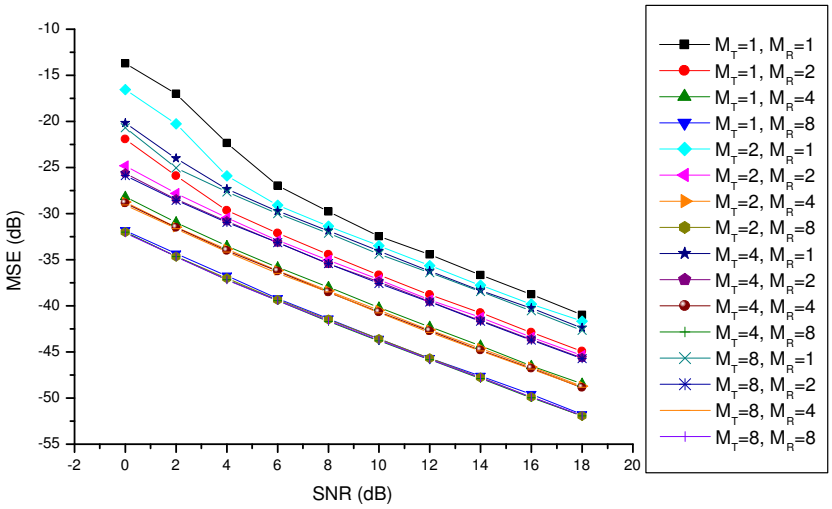

Figure 2.12: MSE performance of generalized moose estimate for two repetitions, true CFO=0.7 subcarrier spacings.

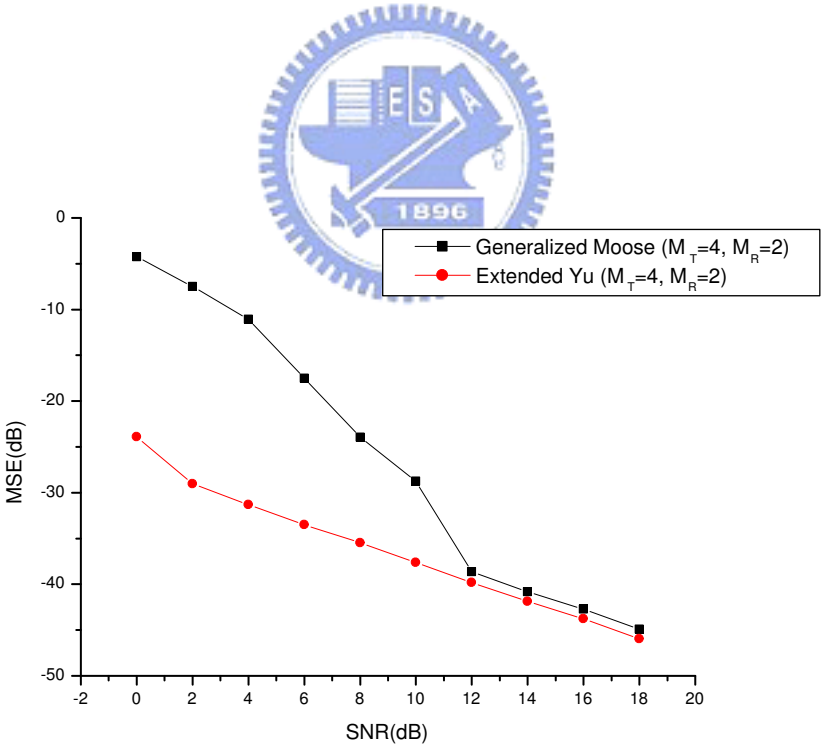

Figure 2.13: MSE performance of CFO estimates for four repetitions, true CFO=0.93 subcarrier spacings.

Chapter 3

Carrier Frequency Offset Estimation for OFDM-CDMA Systems

3.1 Introduction

A block diagram of OFDM-CDMA transmitter is shown in Fig. 3.1 where the input information symbol is first converted into P parallel information symbols $(S_{i0}^k, S_{i1}^k, \ldots, S_{iP-1}^k)$, with k denotes the kth user and i refers to the block to which the P parallel information symbols belong. The pth information symbol in the ith block is then multiplied by a spreading code $\{C_q^k, q = 0, 1, ..., Q-1\}$ assigned to the kth user. These $P \times Q$ spread symbols are mapped onto the subcarriers by an N-point inverse discrete Fourier transform (IDFT). In this figure, P/S, CP and DAC represent respectively a parallel-to-serial converter, cyclic prefix and digital-to-analog converter.

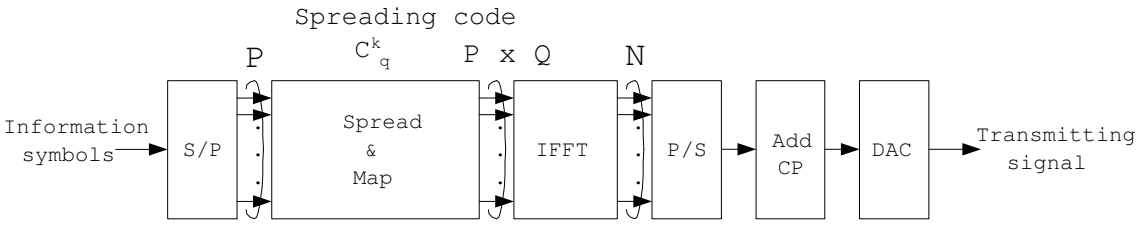

Figure 3.1: Transmitter block diagram of the kth OFDM-CDMA user.

Fig. 3.2 plots the transmit spectra of an OFDM-CDMA signal with virtual subcarriers. The number, N_u, of subcarriers that are modulated by information symbols is

generally smaller than the size of IDFT/DFT to avoid aliasing resulted from oversampling and/or transmit filtering [13], i.e. $N \geq N_u$ in a practical OFDM-CDMA system. All the spread symbols are mapped onto the $P \times Q$ modulated subcarriers by IDFT i.e. $N_u \geq P \times Q$.

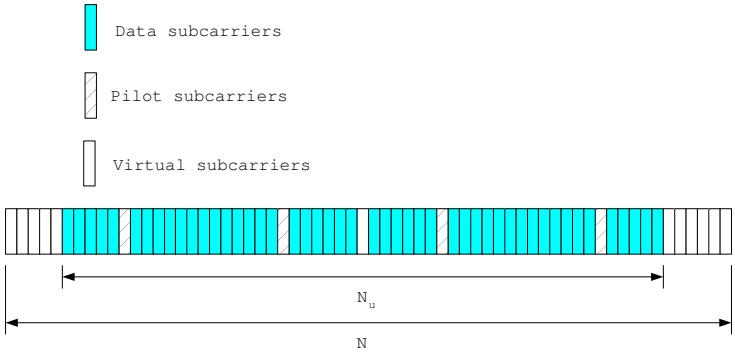

Figure 3.2: Transmit spectra of a typical OFDM-CDMA signal.

Fig. 3.3 and Fig. 3.4 shows two mapping schemes [14]. In the first scheme, the pth parallel information symbol multiplied by the qth chip of the spreading sequence is mapped onto the $(Qp + q)$th subcarrier. We refer to this scheme as a Continuous Mapping (CM) scheme. The second scheme belongs to the class of Discrete Mapping (DM) schemes maps the pth parallel information symbol, multiplied by the qth chip of the spreading sequence, onto the $(p + Pq)$th subcarrier.

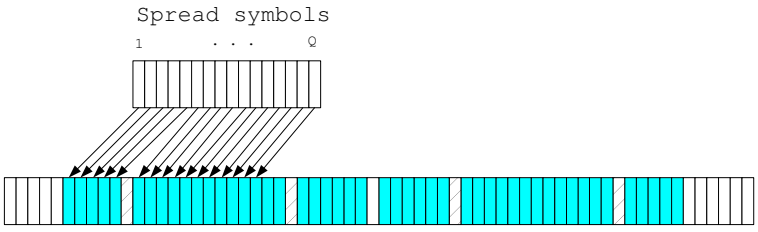

Figure 3.3: A Continuous Mapping (CM) scheme.

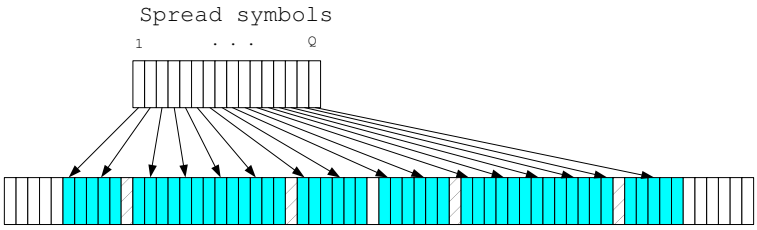

Figure 3.4: A Discrete Mapping (DM) scheme.

3.2 System Model

To begin with, let us consider the special case: $N = N_u = Q$, $P = 1$. Fig. 3.5 plots the OFDM-CDMA transmitter for the kth user. The discrete-time representation of the kth user OFDM-CDMA user is given by

$$d_i^k[n] = \frac{1}{N}\sum_{q=0}^{N-1} S_i^k C_q^k e^{j2\pi nq/N};\ n = 0, 1, ..., N-1;\ i = -\infty, ..., \infty \tag{3.1}$$

where S_i^k is the ith information symbol for the kth user, C_q^k is the qth chip of the the kth user's spreading code of length N which is also equal to the size of the IDFT/DFT pair.

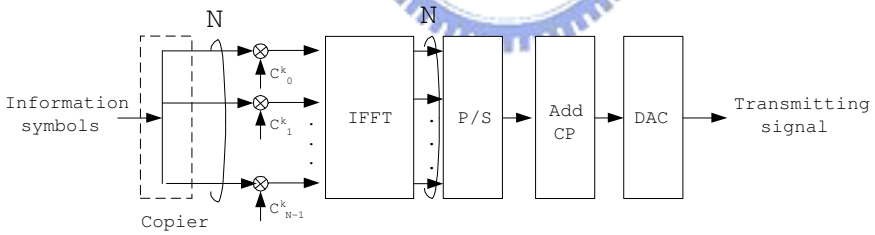

Figure 3.5: Transmitter block diagram of the kth OFDM-CDMA user.

The sequence, $\{d_i^k[n]\}$, after being appended by a cyclic prefix of N_g samples, is transmitted over a multipath fading channel. The length of cyclic prefix is assumed to be greater than or equal to the maximum time spread of the channel. The channel response at the mth subcarrier associated with the kth user is given by

$$H_m^k = \sum_{n=0}^{L-1} h_k[n] e^{-\frac{j2\pi mn}{N}} \tag{3.2}$$

where L is the maximum channel delay of all users and $h_k[n]$ is the nth path of the impulse response associated with the channel between the kth user and the receiver. Shown in Fig. 3.6 is a model for an uplink asynchronous OFDM-CDMA system [15] where each user signal with asynchronous timing and CFO is transmitted over an independent channel.

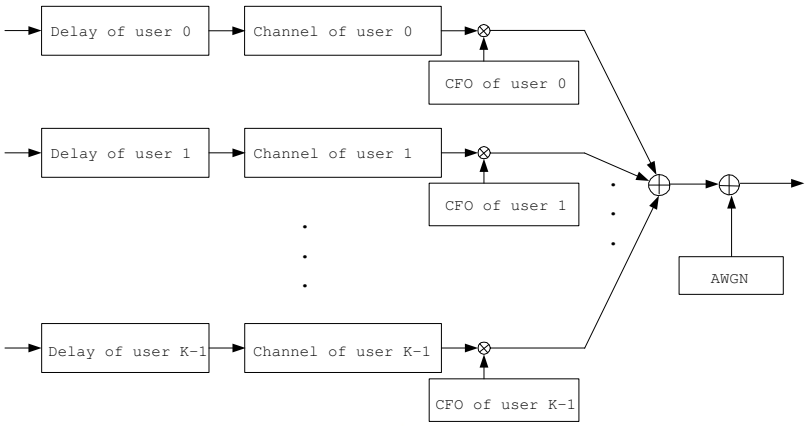

Figure 3.6: An uplink asynchronous OFDM-CDMA transmission model.

The discrete baseband received sample, $y[l]$, at the base station can be expressed as

$$y[l] = \sum_{k=0}^{K-1} \sum_{i=-\infty}^{\infty} r_i^k[l] e^{j2\pi(l-\tau_k)\epsilon_k/N} + w[l] \tag{3.3}$$

where $r_i^k[l]$ is the ith OFDM-CDMA symbol (frame) of the kth user, τ_k is the relative chip delay of the kth user, ϵ_k is the normalized CFO (the actual CFO divided by the intercarrier spacing) of the kth user and $w[l]$ is the complex additive white Gaussian noise (AWGN). The nth chip sample of the ith OFDM-CDMA frame (block) associated with the kth user, $r_i^k[l]$, is

$$r_i^k[n]|_{l=i(N+N_g)+n+\tau_k+N_g} = S_i^k \frac{1}{N} \sum_{q=0}^{N-1} H_q^k C_q^k e^{j2\pi nq/N};\ n = 0, 1, ..., N-1. \tag{3.4}$$

Assuming that the desired user is the dth user and the corresponding timing reference has been established, then we have

$$\begin{aligned} y_i^d[n] &= y[l]|_{l=i(N+N_g)+n+\tau_d+N_g} \\ &= y_i^D[n] + y_i^{MUI}[n] + w_i[n] \end{aligned} \tag{3.5}$$

where we have decompose the received sample into the desired signal component

$$\begin{aligned} y_i^D[n] &= S_i^d e^{j2\pi i(N+N_g)\epsilon_d/N} \frac{1}{N} \sum_{q=0}^{N-1} H_q^d C_q^d e^{j2\pi nq/N} e^{j2\pi n\epsilon_d/N} \\ &\stackrel{def}{=} \widetilde{S}_i^d \frac{1}{N} \sum_{q=0}^{N-1} H_q^d C_q^d e^{j2\pi n(q+\epsilon_d)/N} \end{aligned} \tag{3.6}$$

which we define $\widetilde{S}_i^d = S_i^d e^{j2\pi i(N+N_g)\epsilon_d/N}$, the multiple user interference

$$y_i^{MUI}[n] = \sum_{\substack{k=0 \\ k\neq d}}^{K-1} \sum_{i=-\infty}^{\infty} r_i^k[l] e^{j2\pi(l-\tau_k)\epsilon_k/N}|_{l=i(N+N_g)+n+\tau_d+N_g} \tag{3.7}$$

and white Gaussian noise

$$w_i[n] = w[l]|_{l=i(N+N_g)+n+\tau_d+N_g}. \tag{3.8}$$

Fig. 3.7 is a block diagram of a typical OFDM-CDMA receiver that makes a serial-to-parallel conversion on the received baseband samples and take FFT on each converted block before deriving CFO and channel estimates. The establishment of the timing reference, as mentioned before, is assumed to have been accomplished perfectly whence the corresponding block is not shown for simplicity.

It has been argued [10] that the OFDM-CDMA (MC-CDMA) receiver can use all the received signal energy scattered in the frequency domain while it is difficult for the DS-CDMA receiver to make full use of the received signal energy scattered in the time domain. This is the main advantage of OFDM-CDMA (MC-CDMA) scheme over other multiple access schemes. Taking DFT (FFT) on $\{y_i^d[n]\}$, we obtain

$$\begin{aligned} Y_i^d[m] &= \sum_{n=0}^{N-1} y_i^D[n] e^{-j2\pi nm/N} + \underbrace{\sum_{n=0}^{N-1} (y_i^{MUI}[n] + w_i[n]) e^{-j2\pi nm/N}}_{MUI+AWGN} \\ &= \sum_{n=0}^{N-1} \left(\widetilde{S}_i^d \frac{1}{N} \sum_{q=0}^{N-1} H_q^d C_q^d e^{j2\pi n(q+\epsilon_d)/N} \right) e^{-j2\pi nm/N} + MUI + AWGN \\ &= \widetilde{S}_i^d \sum_{q=0}^{N-1} H_q^d C_q^d \left(\frac{1}{N} \sum_{n=0}^{N-1} e^{j2\pi n\epsilon_d/N} e^{j2\pi n(q-m)/N} \right) + MUI + AWGN \end{aligned} \tag{3.9}$$

where we have defined

$$b^d_{q-m} = \frac{1}{N}\sum_{n=0}^{N-1} e^{j2\pi n\epsilon_d/N} e^{j2\pi n(q-m)/N}. \tag{3.10}$$

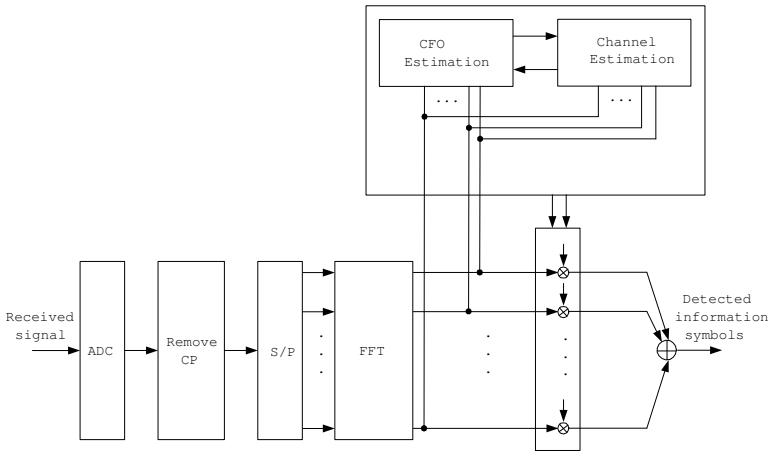

Figure 3.7: Receiver structure for the dth OFDM-CDMA user.

Hence, the mth subcarrier component is given by

$$\begin{aligned} Y^d_i[m] &= \widetilde{S}^d_i \sum_{q=0}^{N-1} H^d_q C^d_q b^d_{q-m} + MUI + AWGN \\ &= \widetilde{S}^d_i H^d_m C^d_m b^d_0 + \underbrace{\widetilde{S}^d_i \sum_{\substack{q=0 \\ q\neq m}}^{N-1} H^d_q C^d_q b^d_{q-m}}_{ICI} + MUI + AWGN \end{aligned} \tag{3.11}$$

and the 1th subcarrier component is

$$\begin{aligned} Y^d_i[1] &= \widetilde{S}^d_i \sum_{q=0}^{N-1} H^d_q C^d_q b^d_{q-1} + MUI + AWGN \\ &= \widetilde{S}^d_i \begin{pmatrix} H^d_0 C^d_0 & H^d_1 C^d_1 & \cdots & H^d_{N-1} C^d_{N-1} \end{pmatrix} \begin{pmatrix} b^d_{-1} = b^d_{N-1} \\ b^d_0 \\ \vdots \\ b^d_{N-2} \end{pmatrix} + MUI + AWGN \\ &= \widetilde{S}^d_i \begin{pmatrix} H^d_1 C^d_1 & H^d_2 C^d_2 & \cdots & H^d_0 C^d_0 \end{pmatrix} \begin{pmatrix} b^d_0 \\ b^d_1 \\ \vdots \\ b^d_{N-1} \end{pmatrix} + MUI + AWGN. \end{aligned} \tag{3.12}$$

Stacking each subcarrier at the output of the FFT block,

$$\mathbf{Y}_i \stackrel{def}{=} [Y_i^d[0]\ Y_i^d[1]\ \cdots\ Y_i^d[N-1]]^T,$$

we obtain

$$\begin{pmatrix} Y_i^d[0] \\ Y_i^d[1] \\ \vdots \\ Y_i^d[N-1] \end{pmatrix} = \widetilde{S}_i^d \begin{pmatrix} H_0^d C_0^d & H_1^d C_1^d & \cdots & H_{N-1}^d C_{N-1}^d \\ H_1^d C_1^d & H_2^d C_2^d & \cdots & H_0^d C_0^d \\ \vdots & \vdots & \ddots & \vdots \\ H_{N-1}^d C_{N-1}^d & H_0^d C_0^d & \cdots & H_{N-2}^d C_{N-2}^d \end{pmatrix} \begin{pmatrix} b_0^d \\ b_1^d \\ \vdots \\ b_{N-1}^d \end{pmatrix} + MUI + AWGN \tag{3.13}$$

and thus

$$\mathbf{Y}_i = \widetilde{S}_i^d \mathbf{C}_{\mathcal{H}}^d \mathbf{b}^d + MUI + AWGN. \tag{3.14}$$

The coefficient vector, $\mathbf{b}^d$, can be decomposed into FFT matrix and the frequency offset vector

$$\begin{pmatrix} b_0^d \\ b_1^d \\ \vdots \\ b_{N-1}^d \end{pmatrix} = \frac{1}{N} \begin{pmatrix} 1 & 1 & \cdots & 1 \\ 1 & e^{j2\pi 1/N} & \cdots & e^{j2\pi(N-1)/N} \\ \vdots & \vdots & \ddots & \vdots \\ 1 & e^{j2\pi(N-1)/N} & \cdots & e^{j2\pi(N-1)^2/N} \end{pmatrix} \begin{pmatrix} 1 \\ e^{j2\pi\epsilon_d/N} \\ \vdots \\ e^{j2\pi(N-1)\epsilon_d/N} \end{pmatrix} \tag{3.15}$$

for

$$\begin{aligned} b_q^d &= \frac{1}{N} \sum_{n=0}^{N-1} e^{j2\pi n\epsilon_d/N} e^{j2\pi nq/N} \\ &= \frac{1}{N} \begin{pmatrix} 1 & e^{j2\pi 1q/N} & \cdots & e^{j2\pi(N-1)q/N} \end{pmatrix} \begin{pmatrix} 1 \\ e^{j2\pi\epsilon_d/N} \\ \vdots \\ e^{j2\pi(N-1)\epsilon_d/N} \end{pmatrix}. \end{aligned} \tag{3.16}$$

Substituting the matrix form

$$\mathbf{b}^d = \mathbf{W}\mathbf{s}(\epsilon_d) \tag{3.17}$$

into (3.14), we obtain

$$\mathbf{Y}_i = \widetilde{S}_i^d \mathbf{C}_{\mathcal{H}}^d \mathbf{W}\mathbf{s}(\epsilon_d) + MUI + AWGN \tag{3.18}$$

where $\mathbf{C}_{\mathcal{H}}^{d}$ is $N \times N$ effective channel spreading matrix for desired user given by

$$\mathbf{C}_{\mathcal{H}}^{d} = \begin{pmatrix} H_0^d C_0^d & H_1^d C_1^d & \cdots & H_{N-1}^d C_{N-1}^d \\ H_1^d C_1^d & H_2^d C_2^d & \cdots & H_0^d C_0^d \\ \vdots & \vdots & \ddots & \vdots \\ H_{N-1}^d C_{N-1}^d & H_0^d C_0^d & \cdots & H_{N-2}^d C_{N-2}^d \end{pmatrix}. \tag{3.19}$$

For the special case of no fading, we have

$$\mathbf{Y}_i = \widetilde{S}_i^d \mathbf{C}_{\mathcal{W}}^d \mathbf{W}\mathbf{s}(\epsilon_d) + MUI + AWGN \tag{3.20}$$

where $\mathbf{C}_{\mathcal{W}}^{d}$ is $N \times N$ spreading matrix for desired user and given by

$$\mathbf{C}_{\mathcal{W}}^{d} = \begin{pmatrix} C_0^d & C_1^d & \cdots & C_{N-1}^d \\ C_1^d & C_2^d & \cdots & C_0^d \\ \vdots & \vdots & \ddots & \vdots \\ C_{N-1}^d & C_0^d & \cdots & C_{N-2}^d \end{pmatrix}. \tag{3.21}$$

3.3 CFO Estimation

Linear-filtering the frequency domain samples $\mathbf{Y}_i$ by the regression vector $\mathbf{V}$, we obtain the associated output energy

$$E[|\mathbf{V}^H \mathbf{Y}_i|^2] = \mathbf{V}^H E[\mathbf{Y}_i \mathbf{Y}_i^H] \mathbf{V} = \mathbf{V}^H \mathbf{R}_{YY} \mathbf{V} \tag{3.22}$$

where $\mathbf{R}_{YY} = E[\mathbf{Y}_i \mathbf{Y}_i^H]$ and $(\cdot)^H$ denote conjugate transpose (Hermitian) of the argument. The following constrained optimization problem

$$\mathbf{V}_{opt}(\epsilon) = arg \min_{V} E[|\mathbf{V}^H \mathbf{Y}_i|^2] \tag{3.23}$$

subject to the constrain

$$\mathbf{V}^H \mathbf{C}_{\mathcal{H}}^d \mathbf{W}\mathbf{s}(\epsilon) = 1 \tag{3.24}$$

can be easily solved by invoking Lagrange multiplier method to obtain

$$\nabla_{\mathbf{V}}(\mathbf{V}^H \mathbf{R}_{YY} \mathbf{V}) - \lambda \nabla_{\mathbf{V}}(\mathbf{V}^H \mathbf{C}_{\mathcal{H}}^d \mathbf{W}\mathbf{s}(\epsilon) - 1) = 0, \tag{3.25}$$

which leads to

$$2\mathbf{R}_{YY}\mathbf{V} = \lambda 2\mathbf{C}_{\mathcal{H}}^{d}\mathbf{W}\mathbf{s}(\epsilon). \tag{3.26}$$

Assume $\mathbf{R}_{YY}$ is nonsingular, we have

$$\mathbf{V} = \lambda\mathbf{R}_{YY}^{-1}\mathbf{C}_{\mathcal{H}}^{d}\mathbf{W}\mathbf{s}(\epsilon) \tag{3.27}$$

where

$$\lambda = \frac{1}{(\mathbf{C}_{\mathcal{H}}^{d}\mathbf{W}\mathbf{s}(\epsilon))^{H}\mathbf{R}_{YY}^{-1}\mathbf{C}_{\mathcal{H}}^{d}\mathbf{W}\mathbf{s}(\epsilon)}. \tag{3.28}$$

Therefore,

$$\begin{aligned}\mathbf{V}_{opt}(\epsilon) &= \frac{\mathbf{R}_{YY}^{-1}\mathbf{C}_{\mathcal{H}}^{d}\mathbf{W}\mathbf{s}(\epsilon)}{(\mathbf{C}_{\mathcal{H}}^{d}\mathbf{W}\mathbf{s}(\epsilon))^{H}\mathbf{R}_{YY}^{-1}\mathbf{C}_{\mathcal{H}}^{d}\mathbf{W}\mathbf{s}(\epsilon)} \\ &= \frac{\mathbf{R}_{YY}^{-1}\mathbf{C}_{\mathcal{H}}^{d}\mathbf{W}\mathbf{s}(\epsilon)}{\mathbf{s}^{H}(\epsilon)\mathbf{W}^{H}\mathbf{C}_{\mathcal{H}}^{dH}\mathbf{R}_{YY}^{-1}\mathbf{C}_{\mathcal{H}}^{d}\mathbf{W}\mathbf{s}(\epsilon)}\end{aligned} \tag{3.29}$$

and the minimum output energy (MOE) is given by

$$\begin{aligned}MOE(\epsilon) &= E[|\mathbf{V}_{opt}^{H}(\epsilon)\mathbf{Y}_i|^2] \\ &= \mathbf{V}_{opt}^{H}(\epsilon)\mathbf{R}_{YY}\mathbf{V}_{opt}(\epsilon) \\ &= \frac{(\mathbf{R}_{YY}^{-1}\mathbf{C}_{\mathcal{H}}^{d}\mathbf{W}\mathbf{s}(\epsilon))^{H}\mathbf{R}_{YY}\mathbf{R}_{YY}^{-1}\mathbf{C}_{\mathcal{H}}^{d}\mathbf{W}\mathbf{s}(\epsilon)}{(\mathbf{s}^{H}(\epsilon)\mathbf{W}^{H}\mathbf{C}_{\mathcal{H}}^{dH}\mathbf{R}_{YY}^{-1}\mathbf{C}_{\mathcal{H}}^{d}\mathbf{W}\mathbf{s}(\epsilon))^{2}} \\ &= \frac{1}{\mathbf{s}^{H}(\epsilon)\mathbf{W}^{H}\mathbf{C}_{\mathcal{H}}^{dH}\mathbf{R}_{YY}^{-1}\mathbf{C}_{\mathcal{H}}^{d}\mathbf{W}\mathbf{s}(\epsilon)}.\end{aligned} \tag{3.30}$$

Since the weighting vector $\mathbf{V}_{opt}$ minimizes the filter output energy with a unit gain at the given ϵ, MOE as a function of the CFO ϵ should exhibit a peak in the neighborhood of the correct CFO ϵ_d of desired user. Fig. 3.8 plots a typical normalized MOE(ϵ) as a function of the normalized CFO.

Hence, the desired CFO estimate is then given by

$$\begin{aligned}\hat{\epsilon}_d &= arg\max_{\epsilon}\{E[|\mathbf{V}_{opt}^{H}(\epsilon)\mathbf{Y}_i|^2]\} \\ &= arg\min_{\epsilon}\{\mathbf{s}^{H}(\epsilon)\mathbf{W}^{H}\mathbf{C}_{\mathcal{H}}^{dH}\mathbf{R}_{YY}^{-1}\mathbf{C}_{\mathcal{H}}^{d}\mathbf{W}\mathbf{s}(\epsilon)\}.\end{aligned} \tag{3.31}$$

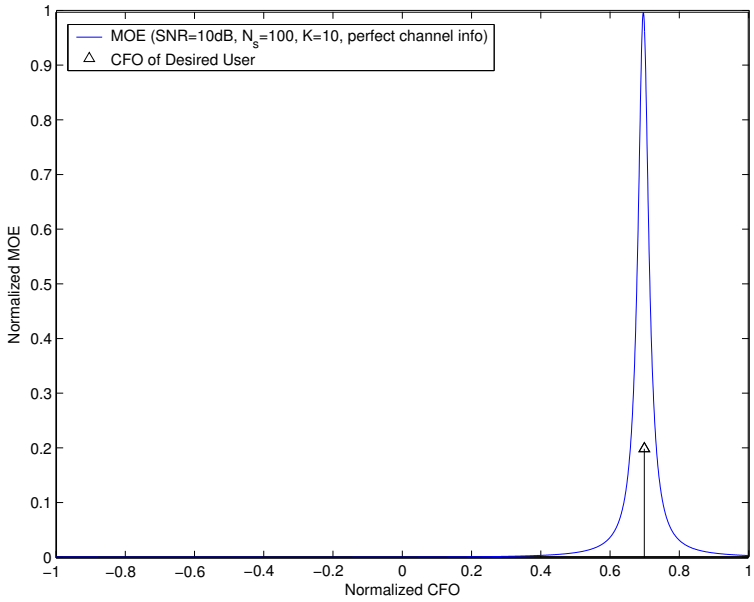

Figure 3.8: Normalized MOE vs Normalized CFO where MOE is normalized by its peak value and the true CFO = 0.7 subcarrier spacings.

Using the correlation ergodicity assumption

$$\widehat{\mathbf{R}}_{YY} \rightarrow \mathbf{R}_{YY}, N_s \rightarrow \infty, \tag{3.32}$$

the data correlation matrix can be approximated by time-averaging over N_s snapshots

$$\widehat{\mathbf{R}}_{YY} = \frac{1}{N_s}\sum_{i=1}^{N_s}\mathbf{Y}_i\mathbf{Y}_i^H. \tag{3.33}$$

However, the CFO estimate requires an exhaustive search over the entire uncertainty range. The resulting complexity may make its implementation infeasible. We observe that $\mathbf{s}(\epsilon)$ has a special structure that can be of use to reduce the complexity of searching the desired CFO solution. Define

$$\widehat{\mathbf{R}}_{ZZ} = \mathbf{W}^H\mathbf{C}_{\mathcal{H}}^{dH}\widehat{\mathbf{R}}_{YY}^{-1}\mathbf{C}_{\mathcal{H}}^{d}\mathbf{W} \tag{3.34}$$

then

$$\hat{\epsilon}_d = arg\min_{\epsilon}\{\mathbf{s}^H(\epsilon)\widehat{\mathbf{R}}_{ZZ}\mathbf{s}(\epsilon)\}. \tag{3.35}$$

The Root MUSIC algorithm, [16], [17] suggests that we set $z = e^{j2\pi\epsilon/N}$ and define the parametric vector

$$\mathbf{s}(z) \quad = \quad \left[1, z, z^2, \cdots, z^{N-1}\right]^T \tag{3.36}$$

so that $\mathbf{s}(z)^H \widehat{\mathbf{R}}_{ZZ} \mathbf{s}(z)$ can be expressed as a polynomial of order $2N-1$,

$$\Lambda(z) \stackrel{def}{=} \mathbf{s}(z)^H \widehat{\mathbf{R}}_{ZZ} \mathbf{s}(z) = \sum_{n=-(N-1)}^{N-1} s(n) z^n \tag{3.37}$$

where $s(n) = \sum_{i,j} \hat{R}_{ZZ}(i,j)$, for $n = j - i$, and $n = -N+1, \cdots, N-1$. As $\Lambda(z)$ is a real smooth function of ϵ, taking derivative of $\Lambda(e^{j2\pi\epsilon/N})$ with respect to ϵ and setting $\partial\Lambda(e^{j2\pi\epsilon/N})/\partial\epsilon \stackrel{def}{=} \dot{\Lambda}(\epsilon) = 0$, we obtain

$$F(z) - F^*(z) = 0, \tag{3.38}$$

where $F(z) = \sum_{n=1}^{N-1} n s(n) z^n$ is a polynomial of order $N-1$. Let $\mathcal{Z} \stackrel{def}{=} \{z_i\}$ be the nonzero complex roots of $F(z) - F^*(z) = 0$, then the desired estimate is given by

$$\hat{\epsilon}_d = \frac{N}{j2\pi} \ln \hat{z} \tag{3.39}$$

where

$$\hat{z} = arg \min_{z_i \in \mathcal{Z}} \{\mathbf{s}(z)^H \widehat{\mathbf{R}}_{ZZ} \mathbf{s}(z)\}. \tag{3.40}$$

The range of estimator is $\pm\frac{N}{2}$ subcarrier spacing. Fig. 3.9 shows the locations of the normalized roots of the polynomial, including the desired CFO estimate.

We summarize our CFO estimation algorithm as following:

1. Collect N_s received blocks and construct the sample correlation matrix $\hat{R}_{YY}$, $\widehat{\mathbf{R}}_{YY} = \frac{1}{N_s} \sum_{i=1}^{N_s} \mathbf{Y}_i \mathbf{Y}_i^H$ and compute $\widehat{\mathbf{R}}_{ZZ} = \mathbf{W}^H \mathbf{C}_{\mathcal{H}}^{dH} \widehat{\mathbf{R}}_{YY}^{-1} \mathbf{C}_{\mathcal{H}}^{d} \mathbf{W}$ with channel information or $\widehat{\mathbf{R}}_{ZZ} = \mathbf{W}^H \mathbf{C}_{\mathcal{W}}^{dH} \widehat{\mathbf{R}}_{YY}^{-1} \mathbf{C}_{\mathcal{W}}^{d} \mathbf{W}$ without channel information.

2. Calculate the coefficients of $F(z)$ based on $\hat{R}_{ZZ}$ where $F(z) = \sum_{n=1}^{N-1} n s(n) z^n$, $s(n) = \sum_{i,j} \hat{R}_{ZZ}(i,j)$, for $n = j - i$.

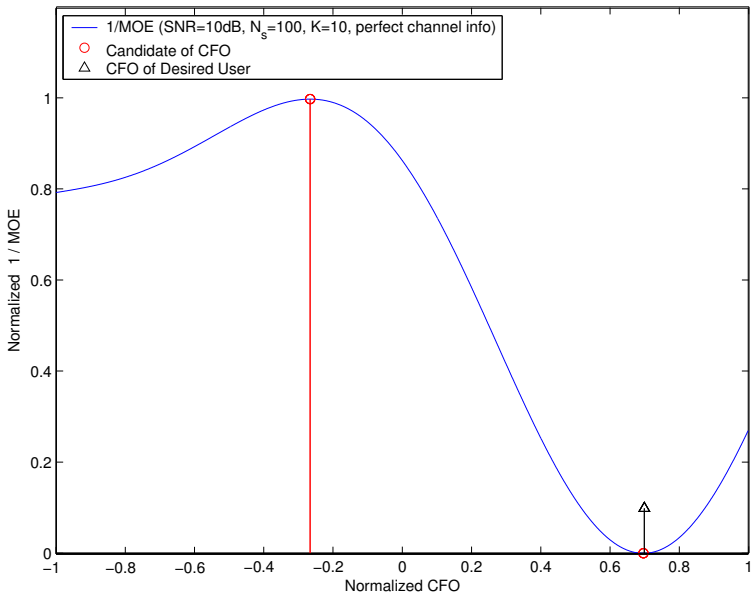

Figure 3.9: Normalized 1/MOE vs Normalized CFO where 1/MOE is normalized by its peak value and the associated root distribution; true CFO = 0.7 subcarrier spacings.

3. Find the nonzero roots of $F(z) - F^*(z) = 0$ and discard undesired roots which outside of CFO estimate range.

4. Obtain the CFO estimate from $\hat{\epsilon}_d = \frac{N}{j2\pi} \ln \hat{z}$ and $\hat{z} = arg\min_{z_i}\{\mathbf{s}(z)^H \widehat{\mathbf{R}}_{ZZ}\mathbf{s}(z)\}$, $z = e^{j2\pi\epsilon/N}$.

3.4 Simulation Results and Discussion

We use the data format of the IEEE 802.11a standard with a sample interval of 50 ns in our simulations. As mentioned before, CFO is normalized by subcarrier spacing. Two static frequency-selective fading channel whose power delay profiles have sixteen exponentially decaying paths and rms delay spreads of 50 ns and 150 ns, respectively, are considered. The former channel is referred to as Model A while the latter is referred to as Model B. Typical magnitude squared frequency responses for these two classes of channels are depicted in Figs. 3.10 and 3.11, respectively. Obviously, Channel B is more selective than Channel A. Table I lists the system and channel parameters used in the

simulation. The signal-to-noise (SNR) ratio is defined as the ratio between the desired signal power and the noise power. Perfect power is assumed such that all received user signal powers are the same.

Table I
System and Channel Simulation Parameters

Parameters	Values
Number of subcarriers	64
Length of cyclic prefix	16 samples
OFDM symbol period	64+16 samples
Modulation	QPSK
Spreading code	Random sequence {-1,1}
Length of spreading Code	64
Channel model	(i) AWGN
	(ii) Frequency selective fading channel 16-path with rms delay spreads of 50 ns (Model A) 16-path with rms delay spreads of 150 ns (Model B)
Power delay profile	Exponential decay
Number of data blocks (N_s)	50, 100, 200
Number of users (K)	10, 30, 50
	All received user signal powers are the same

Fig. 3.12 shows the mean-squared error (MSE) performance of the CFO estimate under various channel conditions. A 10-user asynchronous OFDM-CDMA system is considered and each computer run consists of 100 data blocks. When channel information $\{H_i^d\}$ is not available, the channel estimate is obtained by assuming $\{H_i^d = 1\}$. The performance in channel A without channel information is better than that in channel B because high frequency selective implies low subcarrier correlation and makes it more difficult to distinguish the desired user from the other users via the spreading code. And if the receiver can not distinguish the desired signal from interference, the algorithm tends to cancel the desired signal, eliminating both MUI and part of the desired signal. On the other hand, as expected, when channel information is available the performance under both circumstances improve. The performance in channel B with channel information is better than that in channel A because the more selective channel fading is the larger the distance between the effective channel spreading matrices associated with

different users. In AWGN channels, only the spreading code is available to distinguish different user signals. Fig. 3.13 compares the MSE performance with different number of data blocks. When the data correlation matrix is unknown, we replace the ensemble averages, $\mathbf{R}_{YY}$, for the time averages, $\widehat{\mathbf{R}}_{YY}$. As the number of samples increases, $\widehat{\mathbf{R}}_{YY}$ becomes "closer" to $\mathbf{R}_{YY}$, i.e., if one uses more data blocks for estimating the correlation matrix, the resulting performance will be "closer" to the optimal performance using the true ensemble correlation matrix. The impact of the number of users is plotted in Fig. 3.14 where, as has been expected, it is shown that the MUI power is proportional to the number of system users whose presence degrade the frequency estimate's performance accordingly. Performance of CFO estimate depends mainly on multiuser interference and noise. These performance curves do confirm that the proposed estimator is able to offer reasonable good performance even in a heavily-loaded system. Fig. 3.15 compares the averaged estimate CFO with the true CFO at SNR = 10 dB and shows that as long as the true CFO is within ± 32 (i.e. $\pm N/2$) subcarrier spacings, good estimated values can be obtained.

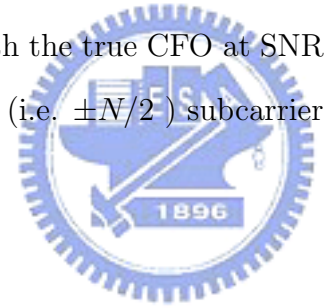

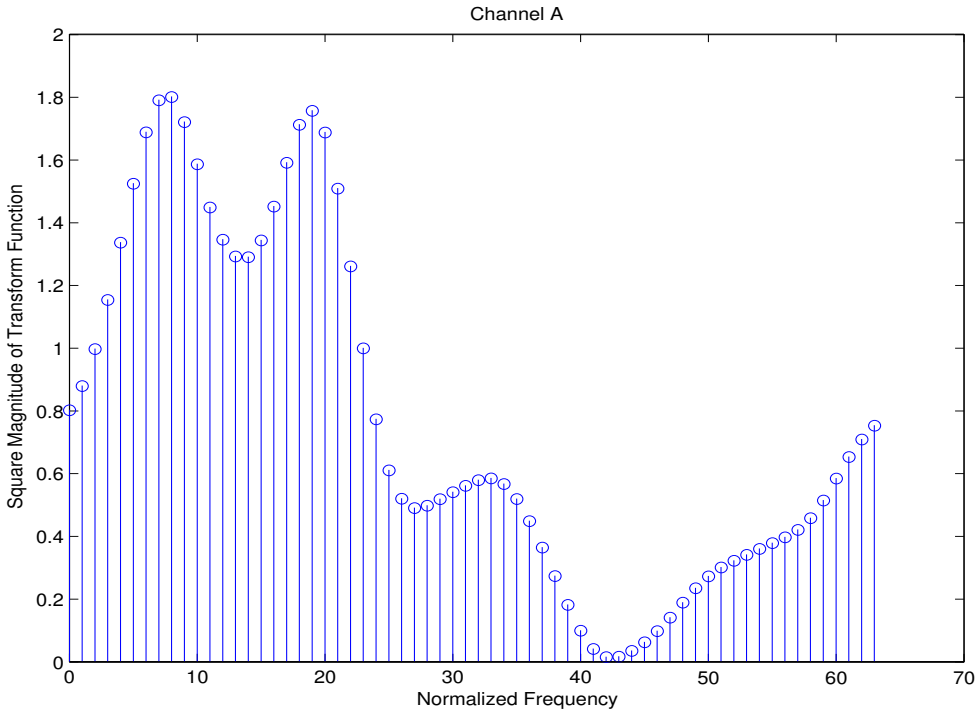

Figure 3.10: Magnitude squared of Channel(Model) A's frequency response.

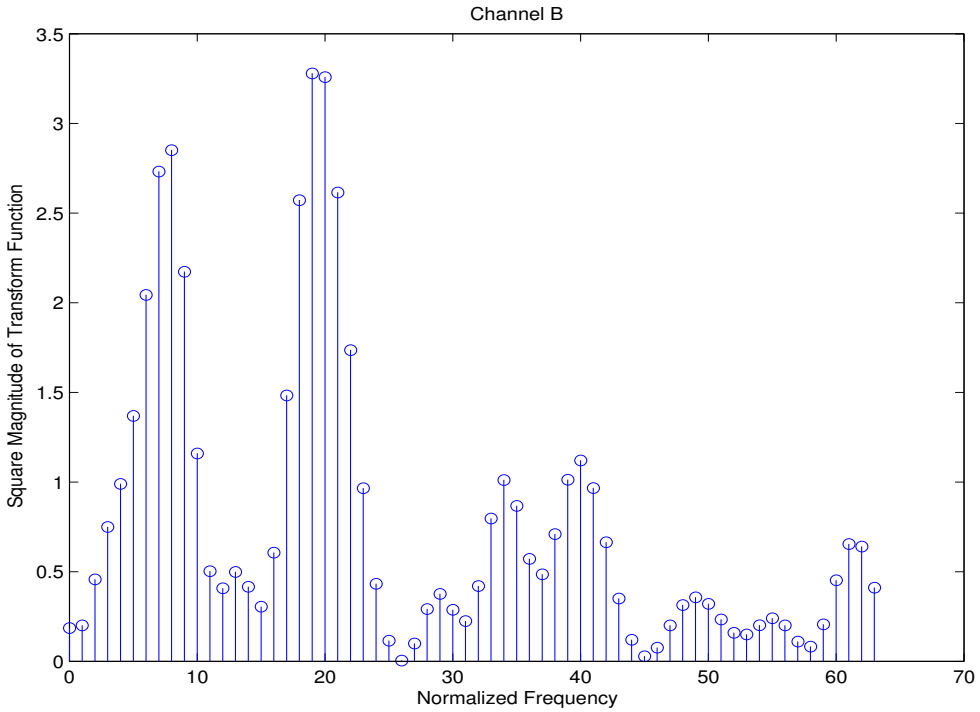

Figure 3.11: Magnitude squared of Channel(Model) B's frequency response.

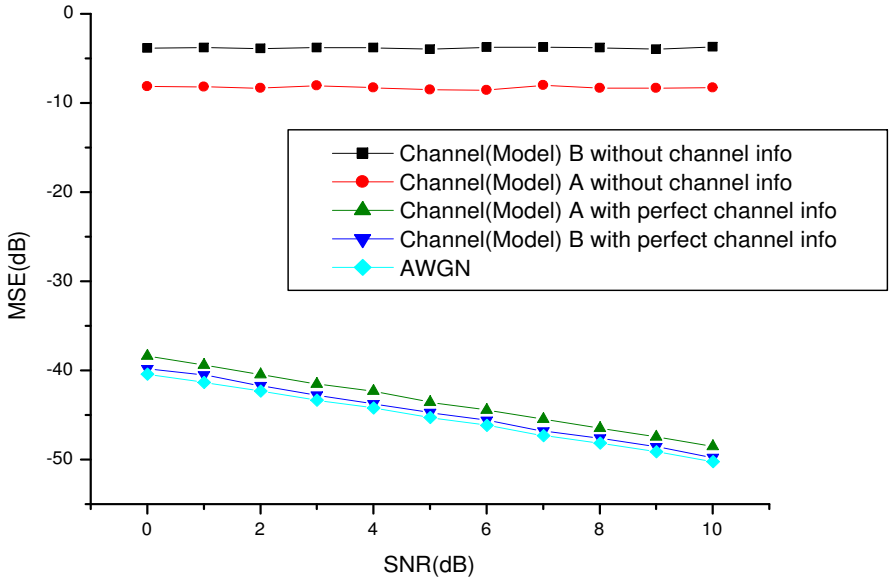

Figure 3.12: MSE performance of CFO estimates for different channel conditions; $K = 10$, $N_s = 100$, true CFO=0.7 subcarrier spacings.

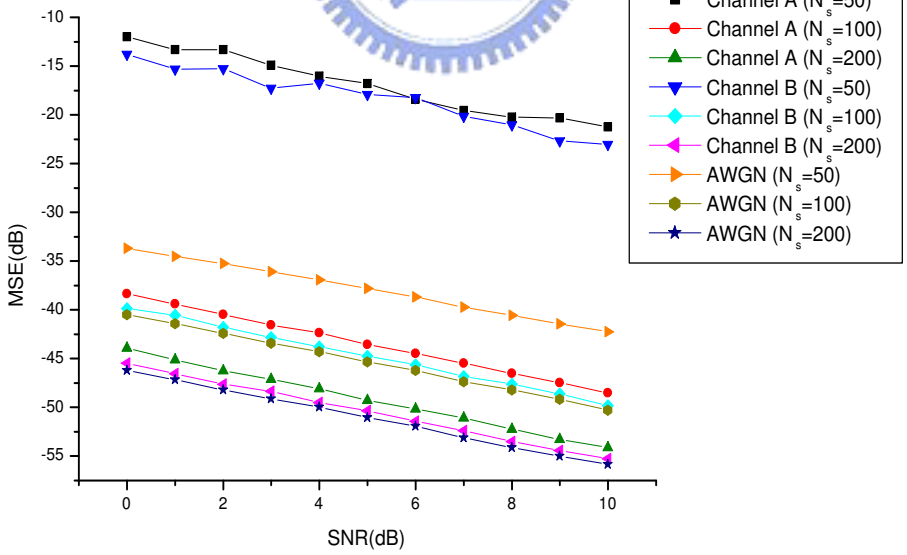

Figure 3.13: MSE performance of CFO estimates for different number of data samples, N_s; $K = 10$, true CFO=0.7 subcarrier spacings, with perfect channel information.

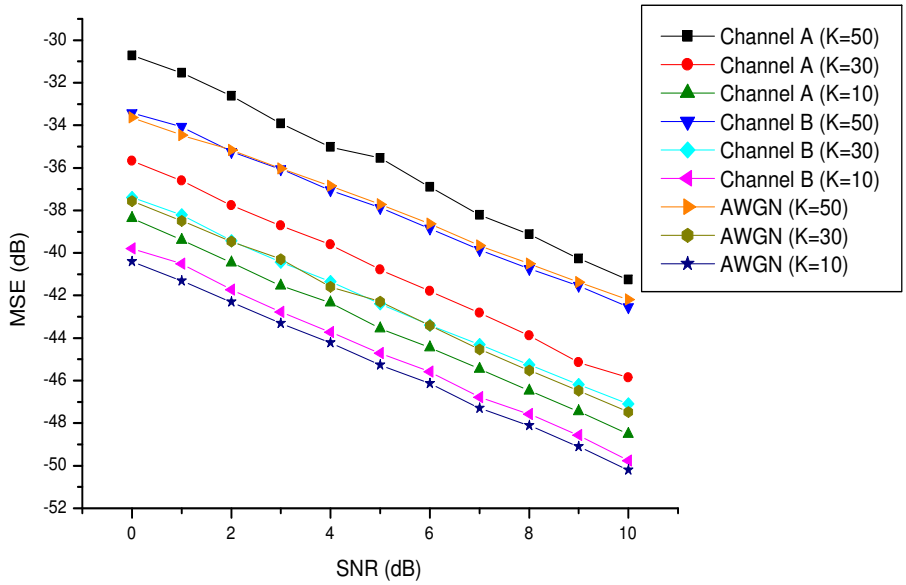

Figure 3.14: MSE performance of CFO estimates for different number of users, K; $N_s = 100$, true CFO=0.7 subcarrier spacings, with perfect channel information.

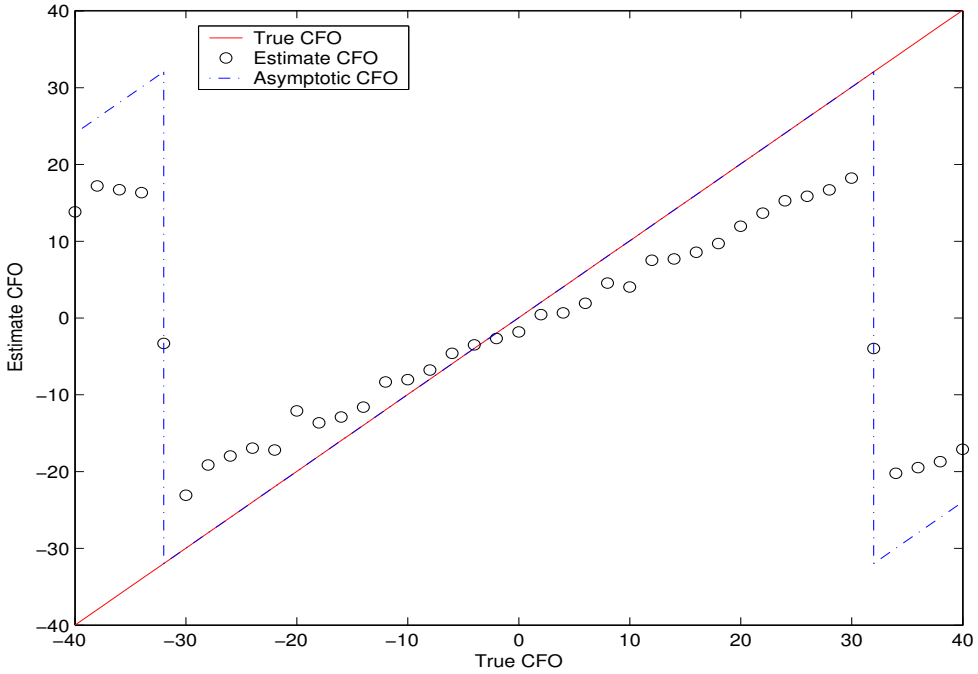

Figure 3.15: Relative CFO estimate versus relative CFO; $K = 10$, $N_s = 500$, with perfect channel information.

3.5 Remarks and Further Discussions

As we have mentioned before, the proposed CFO estimate requires channel information and if this information is not available, the resulting estimate yields poor performance. What we really need is an approach for obtaining CFO and channel estimates simultaneously.

3.5.1 Iterative CFO and channel estimation

Although an optimal joint estimate can be obtained by the generalized maximum likelihood principle the resulting answer is likely to be very complicated. A more practical solution can be obtained through iterative (turbo) processing in which the CFO estimate without channel information serve as an initial estimate in an iterative estimation process. We thus suggest the following two iterative procedures for simultaneous CFO and channel estimation.

Algorithm 1

- Basic assumption: The timing reference of the desired user signal has been successfully established.

1. The initial CFO Estimate, $\hat{\epsilon_d}(p)$, is obtained from

$$\widehat{\mathbf{R}}_{ZZ} = \mathbf{W}^H \mathbf{C}_{\mathcal{W}}^{dH} \widehat{\mathbf{R}}_{YY}^{-1} \mathbf{C}_{\mathcal{W}}^{d} \mathbf{W}$$

2. Derive the channel estimate, $\widehat{H}_m^d(p)$, with the aid of $\hat{\epsilon}_d(p)$.

3. Compute the new CFO estimate, $\hat{\epsilon_d}(p+1)$, using $\widehat{H}_m^d(p)$ and

$$\widehat{\mathbf{R}}_{ZZ} = \mathbf{W}^H \mathbf{C}_{\mathcal{H}}^{dH} \widehat{\mathbf{R}}_{YY}^{-1} \mathbf{C}_{\mathcal{H}}^{d} \mathbf{W}$$

4. Check convergence: $\|\hat{\epsilon_d}(p+1) - \hat{\epsilon_d}(p)\| < \delta \Rightarrow$ go to Step 5; otherwise, set $p = p+1$ and go to Step 2.

5. Output the final estimates, $\hat{\epsilon_d} = \hat{\epsilon_d}(p+1)$ and $\widehat{H}_m^d = \widehat{H}_m^d(p)$.

Under the same assumption, one can also starts with an initial channel estimate and proceed to find the CFO.

Algorithm 2

1. An initial channel estimate, $\widehat{H}_m^d(p)$, is obtained via some blind approach.

2. Obtain the initial CFO estimate, $\hat{\epsilon_d}(p)$, with the help of $\widehat{H}_m^d(p)$ and

$$\widehat{\mathbf{R}}_{ZZ} = \mathbf{W}^H \mathbf{C}_{\mathcal{H}}^{dH} \widehat{\mathbf{R}}_{YY}^{-1} \mathbf{C}_{\mathcal{H}}^{d} \mathbf{W}$$

3. An improved channel estimate, $\widehat{H}_m^d(p+1)$, is obtained by using $\hat{\epsilon}_d(p)$.

4. Convergence check: $\sum_{m=0}^{N-1} \|\widehat{H}_m^d(p+1) - \widehat{H}_m^d(p)\| < \delta \Rightarrow$ go to Step 5; otherwise, set $p = p+1$ and go to Step 2.

5. Output the final estimates, $\hat{\epsilon_d} = \hat{\epsilon_d}(p)$ and $\widehat{H}_m^d = \widehat{H}_m^d(p+1)$.

3.5.2 Successive interference cancellation multi-user-detector

The approach we used so far can be categorized as a single-user estimation approach, basically treating the undesired user signals as interference. Another class of solutions is the multiuser estimation approach that tries to estimate all CFOs either sequentially or simultaneously. We suggest a simple approach similar to the so-called successive interference cancellation used in multiuser detection theory. In accordance with conventional terminology, we refer to our solution as a Successive Interference Cancellation Multi-User-Estimate (SIC MUE), which can be briefly summarized as follows.

The SIC MUE Algorithm

Assuming that there are $L > m$ users whose power can be estimated and the data sequences of the m strongest received sequence has been successfully detected.

1. Order the received signal according to their estimated power.

2. Regenerate a copy of the sum of the strongest received m signals.

3. Subtract from the received signal the regenerated copy to obtain a partially-interference-suppressed version of the received sequence.

4. Perform joint CFO and channel estimate on the strongest signal among the remaining $L - m$ ones based on sequence obtained in the previous step.

5. Make a hard decision on this strongest signal after compensating for the CFO and channel distortion.

6. $m \leftarrow m + 1$, if $m \leq L$ go to Step 2; otherwise output all the detected sequences and stop.

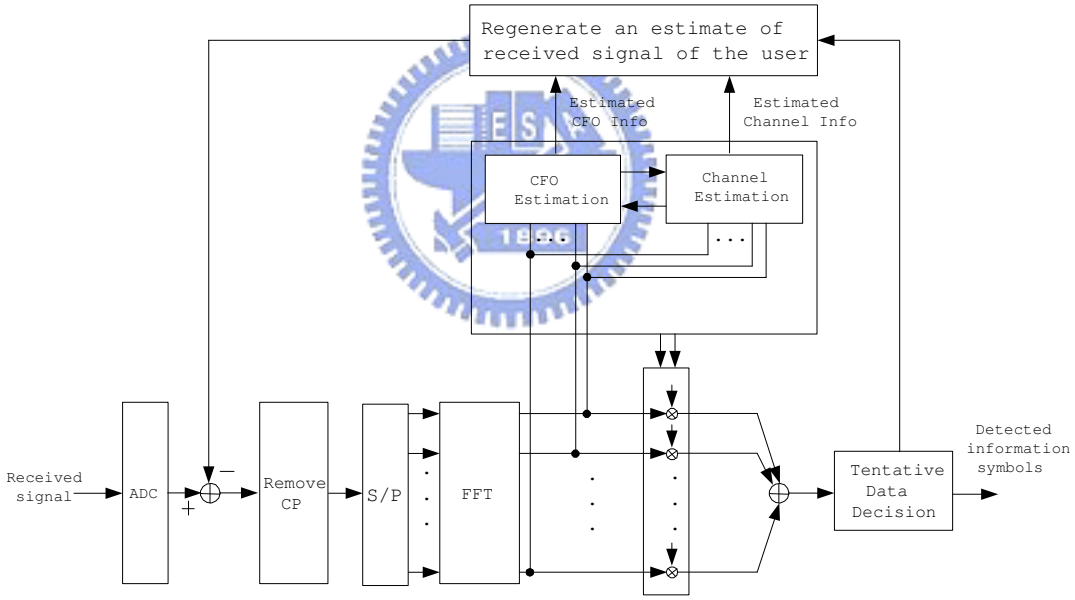

Figure 3.16: An SIC Multiuser detector with iterative CFO and channel estimates.

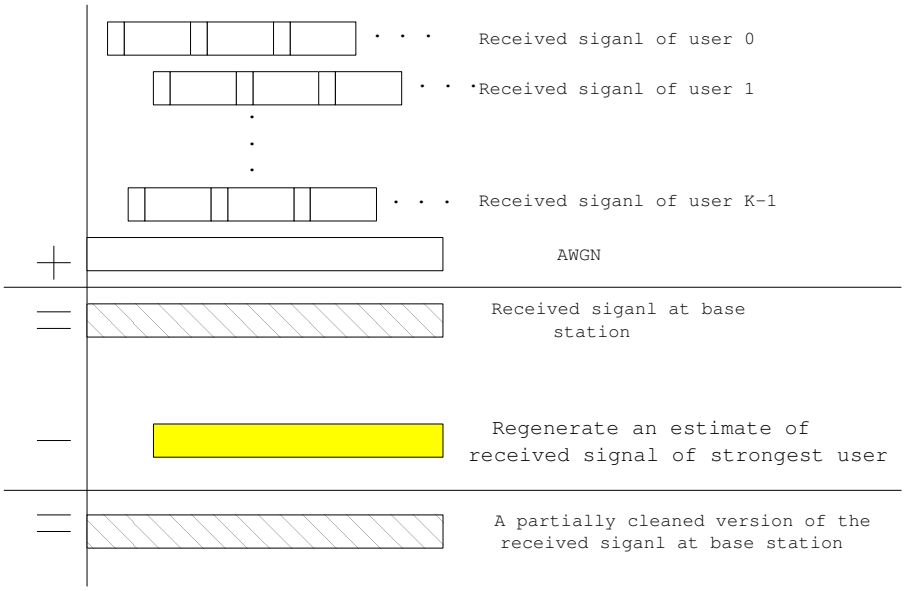

Figure 3.17: An illustration of the SIC MUE concept.

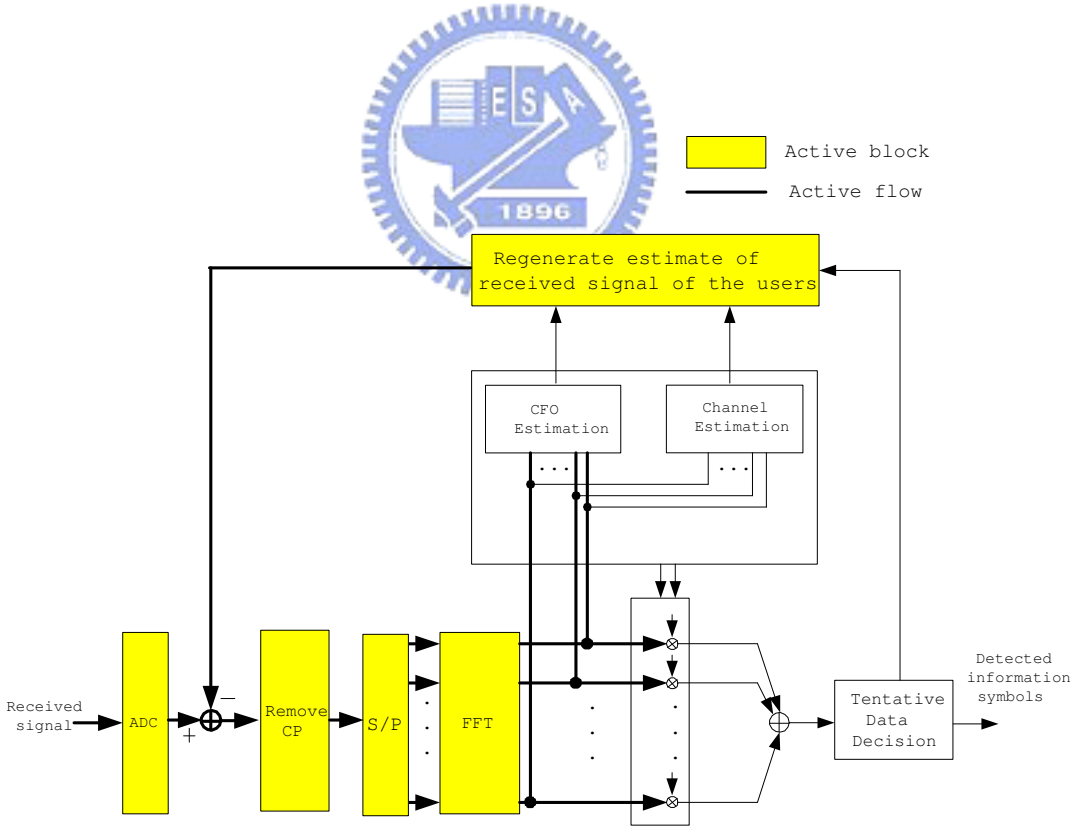

Figure 3.18: Steps 1 - 3 of the SIC MUE algorithm.

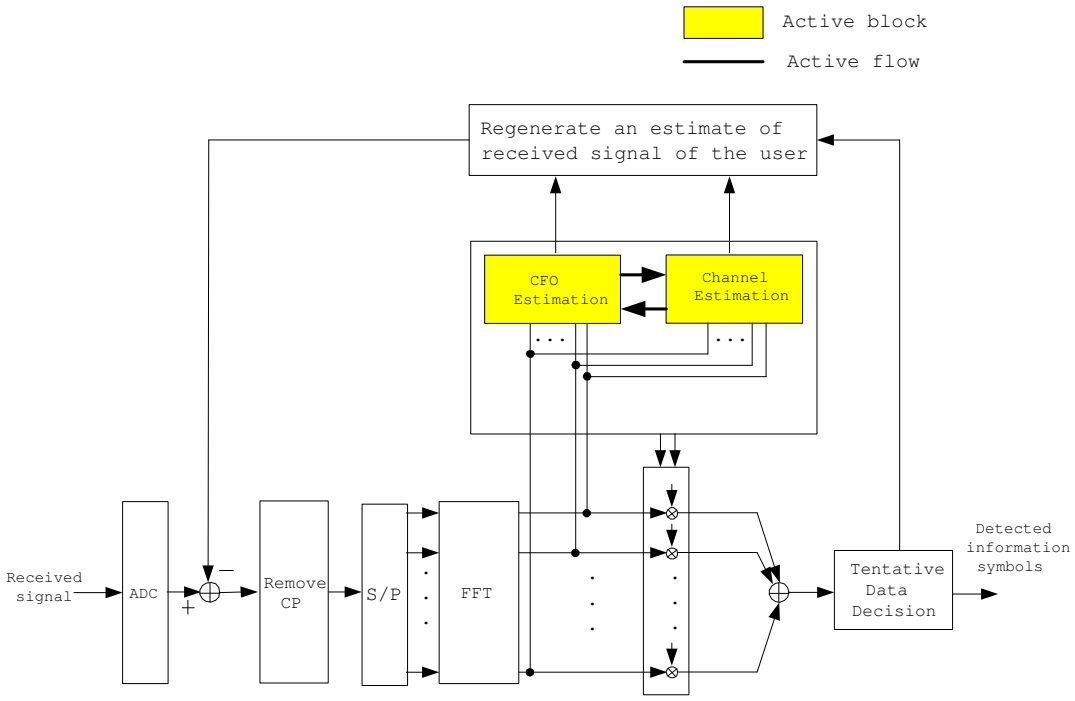

Figure 3.19: Steps 4 of the SIC MUE algorithm.

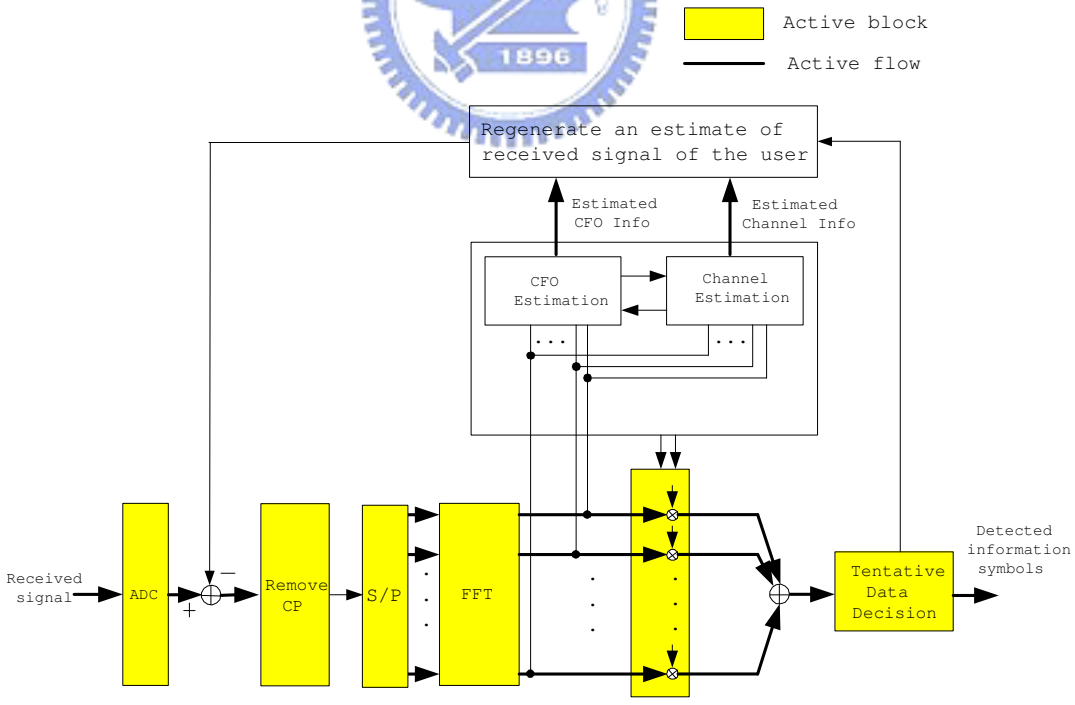

Figure 3.20: Steps 5 and 6 of the SIC MUE algorithm.

Chapter 4

Conclusions

We have extended both Moose's and Yu's maximum likelihood CFO estimation algorithms for use in MIMO-OFDM systems. As long as the length of cyclic prefix is greater than or equal to the maximum delay that accounts for the all users' timing ambiguities and channel multipath delays. The performance of both CFO estimates improves as the number of transmit/receive antennas increases. In other words, the presence of multiple antenna not only promise great capacity enhancement but entail performance improvement for the associated frequency synchronization subsystem.

The frequency synchronization problem for asynchronous OFDM-CDMA systems in frequency selective fading channels is also studied. Assuming frame synchronization has been established and channel estimation is available, we employ a constrained minimum output energy (MOE) criterion for estimating the CFO. The estimate is obtained by searching for the value that yields the largest MOE. Following an approach similar to Yu's ML algorithm, we convert the min/max search into a polynomial rooting problem. The range of the proposed estimate is $\pm\frac{N}{2}$ subcarrier spacings where N is the frame (DFT) size. Performance depends mainly on multiuser interference, thermal noise and number of pilot blocks.

When no channel information is available, the proposed CFO estimate deteriorates and thus some joint frequency and channel estimation scheme is urgently needed. Iterative solutions are suggested but have not been proved. Besides, the proposed solutions

belong to the class of blind estimates that require a relatively long convergence period. It would be very much welcome if we can find either an improved–less complicated and/or faster convergence rate–blind estimate or a pilot-assisted solution with little or no learning period. A joint timing-frequency-channel estimation algorithm for OFDM-CDMA systems is called for as well.

Bibliography

[1] S. Weinstein, P. Ebert, "Data Transmission by Frequency-Division Multiplexing Using the Discrete Fourier Transform," *IEEE Trans. Commun.*, vol. 19, pp. 628 - 634, Oct 1971.

[2] R. van Nee, G. Awater, M. Morikura, H. Takanashi, M. Webster, and K. Halford, "New high-rate wireless LAN standards," *IEEE Commun. Mag.*, vol. 37, pp. 82-88, Dec. 1999.

[3] T. Pollet, M. Van Bladel, M. Moeneclaey, "BER sensitivity of OFDM systems to carrier frequency offset and Wiener phase noise," *IEEE Trans. Commun.*, vol. 43, pp. 191 - 193, Feb./March/April 1995.

[4] P. H. Moose, "A technique for orthogonal frequency division multiplexing frequency offset correction," *IEEE Trans. Commun.*, vol. 42, pp. 2908-2914, Oct. 1994.

[5] T. M. Schmidl and D. C. Cox, "Robust frequency and timing synchronization for OFDM," *IEEE Trans. Commun.*, vol. 45, pp. 1613-1621, Dec. 1997.

[6] M. Morelli, A. N. DAndrea, and U. Mengali, "Frequency ambiguity resolution in OFDM system," *IEEE Commun. Lett.,* vol. 4, pp. 134-136, Apr. 2000.

[7] A.N. Mody, G.L. Stuber, "Synchronization for MIMO OFDM systems," *IEEE Global Telecom.,* vol. 1, pp. 25-29, Nov. 2001.

[8] A.N. Mody, G.L. Stuber, "Receiver implementation for a MIMO OFDM system," *IEEE Global Telecom.,* vol. 1, pp. 17-21, Nov.2002.

[9] Y. Asai, S. Kurosaki, T. Sugiyama, M. Umehira, "Precise AFC scheme for performance improvement of SDM-COFDM," *IEEE Vehicular Tech.,* vol. 3, pp. 24-28, Sept. 2002.

[10] R. Prasad, S. Hara, "An overview of multi-carrier CDMA," *IEEE Spread Spectrum Tech.,* vol. 1, pp. 107 - 114, Sept. 1996.

[11] S. Hara, R. Prasad, "Design and performance of multicarrier CDMA system in frequency-selective Rayleigh fading channels," *IEEE Vehicular Tech.,* vol. 48, pp. 1584 - 1595, Sept. 1999.

[12] S. Tsumura, S. Hara, "Design and performance of quasi-synchronous multi-carrier CDMA system," *IEEE Vehicular Tech.,* vol. 2, pp. 843 - 847, Oct. 2001.

[13] U. Tureli, D. Kivanc, Hui Liu, "MC-CDMA uplink-blind carrier frequency offset estimation," *Signals, Systems and Computers,* vol. 1, pp. 241 - 245 , Nov. 2000.

[14] O. Takyu, T. Ohtsuki, M. Nakagawa, "Frequency offset compensation with MMSE-MUD for multi-carrier CDMA in quasi-synchronous uplink," *IEEE Communications.,* vol. 4, pp. 2485 - 2489, May 2003.

[15] Bangwon Seo, Hyung-Myung Kim, "Frequency offset estimation and multiuser detection for MC-CDMA systems," *MILCOM,* vol. 2, pp. 804 - 807, Oct. 2002.

[16] Jiun-Hung Yu, "Pilot-Assisted Maximum Likelihood Frequency Offset Estimation for OFDM Sytems," thesis, NCTU

[17] H. L. Van Trees, *Optimum Array Processing*, New York: Wiely, 2002.

[18] H. Meyr, M. Moeneclaey, and S. A. Fechtel, *Digital Communication Receivers: Synchronization, Channel Estimation, and Signal Processing*, New York: Wiely, 1997.

簡　　歷

姓　　名：江家賢

居　住　地：台北市

學　經　歷：

2000 年　台灣大學機械工程學系　學士

2004 年　交通大學電信工程學系　碩士

Graduate Courses：

Digital Communications
Random Processes
Digital Signal Processing
Detection and Estimation Theory
Error Control Coding
Array Signal Processing
Adaptive Signal Processing
Special Topic on Digital Communication (Digital Communication Receiver)
Special Topic on Digital Signal Processing